distant-mass contribution is not totally misleading. According to our version of Mach's principle, the effect of a nearby mass m, at distance r, is measured by comparing it with the contribution of the remote universe:

$$\frac{m/r}{M/R}\sim\frac{Gm}{rc^2}. \tag{112}$$

Thus G emerges as a conversion factor between terrestrial standards and cosmical properties.

There are some interesting regularities that position the laboratory between the universe and the atom. With μ of the proton-mass order of magnitude, we note that

$$\frac{M}{1\text{ kg}}\sim\left(\frac{1\text{ kg}}{\mu}\right)^2,\quad \frac{R}{1\text{ cm}}\sim\left(\frac{1\text{ cm}}{\hbar/\mu c}\right)^2, \tag{113}$$

in the sense that the large powers of 10 being compared differ only by small integers. An additional aspect of these empirical scaling laws is expressed by

$$\frac{M}{R^2}\sim\frac{1\text{ kg}}{(1\text{ cm})^2}\sim\frac{\mu}{(\hbar/\mu c)^2}, \tag{114}$$

with a similar understanding concerning small powers of 10. A very suggestive consequence is the derived relation

$$\frac{G\mu^2}{R}\sim\frac{\hbar^2}{\mu R^2}, \tag{115}$$

for this can be read as a statement of dynamical equilibrium—the gravitational attraction of two atoms across the universe is balanced by the quantum kinetic energy demanded by localization within the universe. Does the quantum stabilize the cosmos?

PHYSICAL REVIEW VOLUME 173, NUMBER 5 25 SEPTEMBER 1968

Determination of the Nucleon-Nucleon Scattering Matrix. IX. (n,p) Analysis from 7 to 750 MeV*

MALCOLM H. MACGREGOR, RICHARD A. ARNDT,† AND ROBERT M. WRIGHT
Lawrence Radiation Laboratory, University of California, Livermore, California 94550
(Received 11 April 1968)

Papers VII and VIII in this series contained phase-shift analyses of (p,p) data from 0–400 MeV and from 0–750 MeV, respectively. The present paper gives the corresponding (n,p) analyses. In the energy region below 400 MeV, six single-energy analyses were carried out, as well as an energy-dependent analysis. The combined (p,p) plus (n,p) energy-dependent analysis below 400 MeV includes 839 (p,p) data and 912 (n,p) data. With 45 phenomenological parameters representing 14 free isovector phases and 11 free isoscalar phases, we obtain a solution that yields an average χ^2 per datum of 1.08 for the 1751 data. This solution gives a precision fit to the data from 400 down to 4 MeV, and it extrapolates well above 400 MeV. At energies below 50 MeV, we find that the existing (n,p) data are not yet complete enough to permit a unique determination of the isoscalar phases. Single-energy analyses were also carried out at 425 and 630 MeV, as well as a combined (p,p) plus (n,p) energy-dependent analysis from 0 to 750 MeV. The energy-dependent solution, which includes 53 phenomenological parameters that represent 25 free phases, was obtained by fitting 1147 (p,p) data from 23 to 736 MeV and 901 (n,p) data from 14 to 730 MeV. It has an average χ^2 per datum of 1.34 for the 2048 data. However, at energies above 450 MeV, where, as shown in Paper VIII, the isovector amplitudes are not well known, we cannot uniquely define the isoscalar amplitudes. Nevertheless, the restriction on the phases imposed by fitting to experiments near 425 and 630 MeV enables us to sharpen our knowledge of the phase shifts at lower energies. We find that the $^1P_1$ and $^3D_3$ phases exhibit maxima in the magnitudes near 300 MeV, and that the $^1F_3$ phase is monotonic. Second-derivative and error matrices are tabulated for the single-energy solutions at 25, 50, 95, 142, 210, 330, and 425 MeV. These matrices, which represent our phase-shift solutions fitted to 683 (p,p) data and 572 (n,p) data, contain most of the physical content of the entire elastic nucleon-nucleon data collection. Fitting potential models to these matrices is essentially equivalent to fitting directly to the data. Computationally, using the matrices is vastly simpler.

I. INTRODUCTION

IN Paper VII of this series,[1] we published a phase-shift analysis of the (p,p) scattering data below 400 MeV. Paper VIII gave the corresponding analysis when (p,p) data from 400 to 750 MeV are included.[2] The present paper contains the results of our (n,p) analyses. As in the above papers, we first analyze the energy region below 400 MeV, and then we extend the analysis to include data up to 730 MeV.

Papers VII–IX form a self-contained set, and they supersede the results obtained in Papers I–VI. The pres-

* Work performed under the auspices of the U. S. Atomic Energy Commission.
† Present address: Virginia Polytechnic Institute, Blacksburg, Va.
[1] M. H. MacGregor, R. A. Arndt, and R. M. Wright, Phys. Rev. **169**, 1128 (1968).
[2] M. H. MacGregor, R. A. Arndt, and R. M. Wright, Phys. Rev. **169**, 1149 (1968).

ent paper should be read together with Papers VII and VIII. We have minimized duplications among these three papers. For example, the isoscalar ($I=0$) phases quoted in the present paper must often be taken together with corresponding tables of isovector ($I=1$) phases given in Papers VII or VIII.

Section II of the present paper is a discussion of the data selection. We have examined essentially all of the available (n,p) data below 750 MeV. In cases where we had questions about the data, we have contacted the experimentalists involved. We have included in Sec. II a detailed description of how the data were handled and have supplied references to all of the data. Similar information was contained about (p,p) data in Papers VII and VIII, so that these three papers together constitute our treatment of the available (p,p) and (n,p) scattering data below 750 MeV.

Section III gives the results of single-energy analyses at six energies below 400 MeV. These analyses are the extension to isoscalar amplitudes of the corresponding analyses of isovector amplitudes given in Paper VII. Section IV contains the energy-dependent results below 400 MeV. Section V gives the energy-dependent and energy-independent analyses extended above 400 MeV. Since the results of Sec. V are quite meager, we did not feel justified in presenting this work as a separate paper, although it is the (n,p) counterpart of Paper VIII.

In Sec. VI we discuss limitations in the phase-shift analysis, and we compare our results with those of the recent Yale[3] energy-dependent analyses of (p,p) and (n,p) scattering. Section VII contains our conclusions and observations about the present status of nucleon-nucleon phase-shift phenomenology.

II. DATA SELECTION

The method we used in selecting (n,p) elastic scattering data was somewhat different from that used in selecting (p,p) elastic scattering data. In the latter case, as described in Paper VII, we made very careful consistency checks.[1] A bootstrap procedure was used to build up a self-consistent (p,p) data set. Using as a reference the phase-shift solution obtained by fitting to this set, we then reexamined all of the (p,p) data. Individual data that deviated by more than three standard deviations from the reference curves were deleted, and then data sets that deviated on the average by more than two standard deviations were deleted. The final data compilation thus obtained was used to obtain the final (p,p) phase-shift solutions. Of 1084 (p,p) data considered in detail, 839 were included in the final data set. Most of the data rejected were older data, although we removed the Wisconsin (p,p) differential cross-section data[4] from 1.4 to 3 MeV because our vacuum polarization corrections were only approximate. The fit of the final phase-shift solution to the Wisconsin data at 2.425 and 3.037 MeV actually fell well within the statistical limits described above, as shown in Table I of Paper VII.

In the case of (n,p) scattering, the (n,p) data are manifestly incomplete. (n,p) experiments are intrinsically more difficult to perform than (p,p) experiments, and the required triple-scattering and spin-correlation experiments are largely lacking. A "complete set" of elastic (n,p) experiments at one energy consists of five independent observables measured over the full 0°–180° angular range. What we actually have at most energies are two kinds of (n,p) experiments—total- and differential cross-section measurements, and polarization measurements. This being the case, we can analyze the (n,p) data only by using information from (p,p) scattering, together with some assumption about charge independence, which essentially fixes the isotopic spin $I=1$ scattering amplitudes. Then the available (n,p) data can be used to obtain some information about the $I=0$ amplitudes. However, the statistical accuracy of the determination of the $I=0$ amplitudes in this manner is much lower than the accuracy with which the $I=1$ amplitudes are determined, and the systematic errors can be large. Given this situation, we have no reliable way in which to carry out a careful evaluation of the existing (n,p) data. Indeed, since the uncertainties in the $I=0$ amplitudes arise as much or more from the incompleteness of the (n,p) data as from any systematic errors in the existing data, there is not much point at this time in worrying very much about small inconsistencies that may be present in these data.

Our approach in the present work was to keep all of the available (n,p) data except for the few that we know to be very inaccurate, and except for some redundant data that were deleted because of computer space limitations. In Table I is given a listing of the (n,p) data from 7 to 730 MeV, together with comments as to how the data were handled. The references for these data are given in Table II. The data at the starred energies in Table I were used for the energy-independent analyses. A total of 912 data were used for the 0–400-MeV energy-dependent analysis. For the 0–750-MeV energy-dependent analysis, the available (n,p) data above 400 MeV were added, and a few of the low-energy data were removed, as described in Table I.

There were available to us 91 measurements of total cross sections in the energy range below 130 MeV. Of these, 63 were measurements by Bowen and co-workers[5] (BSSTH) at energies from 15.8 to 111.5 MeV. Since it was not convenient for us to treat all of these data directly, we made a computer fit to these data and then used the resulting curve to arbitrarily delete from the BSSTH data 22 points that were more than one standard deviation off the curve. Seventeen of the remaining

[3] R. E. Seamon, K. A. Friedman, G. Breit, R. D. Haracz, J. M. Holt, and A. Prakash, Phys. Rev. **165**, 1579 (1968).

[4] D. J. Knecht, P. F. Dahl, and S. Messelt, Phys. Rev. **148**, 1031 (1966).

[5] P. H. Bowen *et al.*, reference Harwell (1961) of Table II.

TABLE I. (n,p) data from 7 to 730 MeV.

Energy[a] (MeV)	No., type, data	Angular range (c.m.)	Data std. err.	Norm. std. err.	Deleted angles	M value[b]	Predicted norm.[c]	Comment	Reference[d]
7.17	$1\sigma_T$		2%			3.2		e	Livermore (1958)
8.77	$1\sigma_T$		1%			1.7		e	Livermore (1958)
10.42	$1\sigma_T$		2%			6.8		e	Livermore (1958)
11.13	$1\sigma_T$		2%			4.4		e	Livermore (1958)
13.13	$1\sigma_T$		3%			3.7		e	Livermore (1958)
14.02	$1\sigma_T$		2%			17.5		e	Livermore (1958)
14.1	8σ	48°–155°	4%			(0.2)	(0.962)	f	Los Alamos (1953)
14.1	16σ	11°– 93°	8%	Float		0.2	0.995		Haifa (1967)
14.1	6σ	70°–173°	4%	4%		0.2	1.014		Los Alamos (1955A)
14.1	$1\sigma_T$		0.7%			8.4			Brookhaven (1952)
15.7	16σ	56°–162°	5%	Float				f	Glasgow (1967)
15.8 –96.0	σ_T							g	Harwell (1961)
16.4	$1\sigma_T$		3%			1.1		h	Harwell (1961)
16.4	$3P$	100°–140°	50%	9.3%		0.7	0.999		Wisconsin (1962)
17.8	$1\sigma_T$		2%			6.7		e	Livermore (1960)
18.4	$1\sigma_T$		3%			0.0		i	Harwell (1961)
19.6	$1\sigma_T$		0.5%			8.6			Canberra (1966)
19.6	$1\sigma_T$		0.6%			11.9		j	Los Alamos (1955B)
*20.5	$1\sigma_T$		2%			0.0		k	Harwell (1961)
*20.5	$9P$	21°–101°	70%	18.8%		0.7	1.116		Harwell (1965)
*20.6	$1\sigma_T$		2%			0.7		e	Livermore (1960)
*22.5	12σ	65°–175°	4%	Float		0.5	1.011		Los Alamos (1962)
*22.5	6σ	7°– 51°	6%	3.3%		0.7	0.982		Harwell (1963)
*23.1	$6P$	50°–150°	20%	10%		1.0	0.901		Los Alamos (1963)
*23.1	$1P$	140°	50%			3.6			Los Alamos (1966)
*23.1	$4C_{NN}$	130°–174°	30%			0.7			Los Alamos (1966)
23.1	$3D$	70°–110°	30%					l	Los Alamos (1964)
*23.7	$1\sigma_T$		2%			1.0		m	Harwell (1961)
*23.7	$4P$	80°–140°	90%	10.9%		0.7	0.930		Wisconsin (1962)
*23.7	$1\sigma_T$		0.5%			7.8		n	Canberra (1966)
25.3	$1\sigma_T$		2%			4.0		e	Livermore (1960)
*25.9	$1\sigma_T$		3%	2%		1.4	1.012	o	Harwell (1961)
*27.5	8σ	7°– 72°	7%	3%		0.1	0.998		Harwell (1963)
*27.5	3σ	159°–173°	7%	Float		0.9	0.945		Harwell (1963)
*28.0	$1\sigma_T$		0.7%			11.5			Canberra (1966)
28.3	$1\sigma_T$		3%			1.8		e	Livermore (1960)
29.0	$1\sigma_T$		3%			2.8		e	Livermore (1960)
*29.6	$1\sigma_T$		3%	2%		0.0	0.999	o	Harwell (1961)
*30.0	$9P$	21°–101°	50%	8.3%		1.4	0.941		Harwell (1965)
*30.0	$3P$	139°–159°	100%	8.3%		1.1	0.974		Harwell (1965)
32.5	$1\sigma_T$		3%	2%		0.4	1.007	o, p	Harwell (1961)
32.5	9σ	7°– 82°	7%	2.1%		0.7	1.027		Harwell (1963)
32.5	6σ	129°–173°	5%	4%		1.3	0.987		Harwell (1963)
33.1	$1\sigma_T$		3%	2%		0.1	1.005		Harwell (1961)
34.0	$1\sigma_T$		3%	2%		0.2	0.994	o	Harwell (1961)
37.5	10σ	7°– 92°	8%	2%		0.4	1.000	q	Harwell (1963)
37.5	7σ	118°–173°	6%	4%		0.7	0.967	q	Harwell (1963)
38.0	$1\sigma_T$		4%	2.6%		0.8	0.986	o	Harwell (1952B)
38.5	$1\sigma_T$		3%	2%		0.4	0.992	o, q	Harwell (1961)
40.0	$1\sigma_T$		3%	2%		0.0	1.000	r	Harwell (1961)
40.0	$9P$	21°–101°	20%	10.6%		0.8	1.043		Harwell (1965)
40.0	$6P$	109°–159°	25%	10.6%		0.7	1.070		Harwell (1965)
41.1	$1\sigma_T$		3%	2%		0.9	0.989	o	Harwell (1961)
42.0	13σ	62°–180°	5%	3.5%		(3.2)	(0.972)	f	Berkeley (1949)
42.5	11σ	7°–102°	7%	2%		0.8	0.998		Harwell (1963)
42.5	11σ	78°–173°	6%	4%		1.1	0.974		Harwell (1963)
42.5	$1\sigma_T$		3%	2%		1.0	0.988	o	Harwell (1961)
44.0	$1\sigma_T$		3%	2%		0.7	0.990	o	Harwell (1961)
45.5	$1\sigma_T$		8%	2.2%		0.2	1.002	o, s	Harvard (1954A)
45.5	$1\sigma_T$		3%	2%		0.0	1.002	o	Harwell (1961)
*47.5	11σ	7°–102°	7%	2%		0.9	1.006		Harwell (1963)
*47.5	11σ	78°–173°	5%	4%		0.8	0.989		Harwell (1963)
*48.8	$1\sigma_T$		3%	2%		0.6	0.990	o	Harwell (1961)
*50.0	$9P$	21°–101°	10%	4.7%		0.3	1.029		Harwell (1965)
*50.0	$6P$	99°–159°	15%	4.7%	149°	0.8	1.014		Harwell (1965)
*52.5	12σ	7°–112°	7%	1.7%		0.8	1.013		Harwell (1963)
*52.5	11σ	78°–173°	5%	3.8%		0.8	1.015		Harwell (1963)
*52.5	$1\sigma_T$		3%	2%		0.8	0.988	o	Harwell (1961)
*56.6	$1\sigma_T$		2%	2%		0.0	0.997	o	Harwell (1961)
*57.5	12σ	7°–112°	7%	2%		0.6	1.013		Harwell (1963)
*57.5	11σ	78°–173°	5%	4%		1.6	0.989		Harwell (1963)
*58.8	$1\sigma_T$		2%	2%		0.0	1.000	o	Harwell (1961)
*60.0	$9P$	21°–101°	10%	3.9%		1.3	0.927		Harwell (1965)
*60.0	$7P$	99°–159°	10%	3.9%		1.8	0.982		Harwell (1965)
62.5	12σ	7°–112°	7%	2%		1.3	0.989	q	Harwell (1963)
62.5	11σ	78°–173°	6%	4%		1.2	0.949	q	Harwell (1963)

TABLE I. (*continued*).

Energy[a] (MeV)	No., type, data	Angular range (c.m.)	Data std. err.	Norm. std. err.	Deleted angles	M value[b]	Predicted norm.[c]	Comment	Reference[d]
63.0	$1\sigma_T$		3%	1.6%		0.2	1.004	o	Harwell (1952B)
66.1	$1\sigma_T$		2%	2%		0.5	0.990	o	Harwell (1961)
68.9	$1\sigma_T$		2%	2%		0.4	0.992	o	Harwell (1961)
70.0	12σ	7°–122°	6%	2%	112°	1.4	0.996		Harwell (1963)
70.0	11σ	78°–173°	6%	4%		1.6	0.922		Harwell (1963)
70.0	$9P$	21°–101°	10%	3.9%		1.8	0.906	q	Harwell (1965)
70.0	$7P$	98°–159°	20%	3.9%		0.8	0.983	q	Harwell (1965)
72.0	$1\sigma_T$		2%	2%		3.2	0.976	o	Harwell (1961)
77.0	$17P$	20°–159°	10%	8%				t	Harwell (1960)
80.0	12σ	7°–112°	7%	2%	122°	1.9	0.979	q	Harwell (1963)
80.0	11σ	78°–173°	6%	4%		0.8	0.969	q	Harwell (1963)
80.0	$9P$	21°–102°	12%	4.2%		0.7	0.943		Harwell (1965)
80.0	$7P$	98°–159°	15%	4.2%		0.5	1.022		Harwell (1965)
82.8	$1\sigma_T$		2%	2%		2.4	0.979	o	Harwell (1961)
86.9	$1\sigma_T$		2%	2%		0.9	0.988	o	Harwell (1961)
88.0	$1\sigma_T$		2%	2.3%		1.0	1.016	o	Harvard (1954A)
88.0	$1\sigma_T$		2%	2.3%		0.1	1.004	o	Harvard (1954A)
88.0	$1\sigma_T$		2%			2.4		u	Harvard (1966A)
*89.5	13σ	7°–122°	7%	2%		1.5	0.976		Harwell (1963)
*89.5	11σ	78°–173°	6%	4%		1.0	0.963		Harwell (1963)
90.0	19σ	36°–180°	10%	4%		(2.9)	(0.987)	f	Berkeley (1949)
*90.0	$9P$	21°–102°	15%	5.1%		0.8	0.942		Harwell (1965)
*90.0	$7P$	98°–159°	30%	5.1%		0.4	1.014		Harwell (1965)
*91.0	25σ	59°–177°	3%	Float		1.0	0.989		Harvard (1954B)
*91.0	$1\sigma_T$		2%	2%		0.9	0.987	o, v	Harwell (1961)
*95.0	$1\sigma_T$		4%	2%		0.5	0.993	o	Harwell (1952B)
*95.0	$15P$	22°–160°	20%	8%		2.2	0.934		Harwell (1957)
*99.0	$1\sigma_T$		2%			3.5		w	Harvard (1966A)
*99.0	13σ	7°–122°	7%	1.7%		1.5	0.985		Harwell (1963)
*99.0	11σ	78°–173°	6%	3.8%		1.0	1.022		Harwell (1963)
*100	$9P$	21°–102°	15%	7.3%		0.4	1.025		Harwell (1965)
*100	$7P$	98°–159°	30%	7.3%		0.7	1.030		Harwell (1965)
*100	$1\sigma_T$		2%	2%		0.0	0.999	o, x	Harwell (1961)
105	7σ	6°– 62°	10%	8%		0.4	1.100		Oxford (1955)
105	$1\sigma_T$		2%	2%		0.4	1.009	o, y	Harwell (1961)
108.5	13σ	7°–122°	8%	2%		1.4	0.993		Harwell (1963)
108.5	11σ	78°–173°	8%	4%		1.8	1.017		Harwell (1963)
110	$9P$	22°–102°	30%	10%		1.1	1.029	q	Harwell (1965)
110	$7P$	98°–158°	40%	10%		1.5	1.057	q	Harwell (1965)
110	$1\sigma_T$		2%			3.8			Harvard (1966A)
110	$1\sigma_T$		3%	2%		2.4	1.016	o, z	Harwell (1961)
120	$1\sigma_T$		2%			2.5		aa	Harvard (1966A)
120	$9P$	22°–102°	40%	14.9%		0.5	1.021		Harwell (1965)
120	$7P$	98°–159°	60%	14.9%		0.7	1.055		Harwell (1965)
126	$6P$	33°– 82°	8%	10%		0.6	1.080	bb	Harvard (1964B)
126	$1\sigma_T$		4%	1.6%		0.2	0.997	o	Harwell (1952B)
*128	10σ	78°–170°	3%	2.2%		0.5	0.998		Harvard (1960)
*128	$10P$	78°–170°	30%	10%		1.5	1.050	bb	Harvard (1960)
*128	$5D_T$	124°–160°	80%			1.2			Harvard (1962A)
*128	$1D_T$	170°	70%			0.0			Harvard (1964A)
*128.5	$3A_T'$	139°–164°	70%			1.6			Harvard (1967)
*129	15σ	73°–177°	5%	6.5%		0.9	0.974		Harvard (1966B)
*129.4	$1\sigma_T$		3%			1.3			Harvard (1966A)
*130	14σ	25°–155°	15%	3.2%		0.9	0.955		Harwell (1956)
*135	$5A$	42°– 84°	50%	4%		0.6	0.998	cc	Harvard (1962B)
*137	7σ	6°– 62°	10%	5%		0.6	0.977		Oxford (1955)
*137	$5R$	42°– 84°	80%			0.5		cc	Harvard (1962B)
*140	$1\sigma_T$		12%			0.7			Rochester (1952)
*140	$14P$	31°–160°	10%	7%		1.5	1.092	bb, dd	Rutherford (1962)
*140.9	$1\sigma_T$		2%			1.9			Harvard (1966A)
*143	$8P$	41°–118°	5%	Float		1.3	0.906	ee	Harvard (1961)
*150	16σ	63°–177°	4%	6.5%		0.8	0.976		Harvard (1966B)
*150.9	$1\sigma_T$		2%			1.4			Harvard (1966A)
153	19σ	50°–178°	6%	2.2%		(4.8)	(0.974)	f, ff	Harwell (1952A)
*153	$1\sigma_T$		3%	2%		5.4	0.970	o	Harwell (1952B)
156	$1\sigma_T$		17%			0.0			Rochester (1952)
*197	$3D_T$	126°–148°	100%			0.5		cc	Rochester (1967A)
*199	8σ	76°–158°	2%	Float		1.0	0.984		Rochester (1967B)
*199	$8P$	76°–158°	10%	10%		1.0	1.041		Rochester (1967B)
*200	20σ	6°–174°	4%	2.1%	180°	1.4	0.977		Dubna (1963)
*200	$1\sigma_T$		2%			0.9			Dubna (1963)
*203	$5R_T$	139°–179°	20%	14%		0.4		cc	Rochester (1966)
*212	$5D$	40°– 80°	12%			0.6		cc	Rochester (1962)
*217	$6P$	40°– 90°	15%	12%		0.6		cc	Rochester (1961)
260	15σ	37°–180°	15%	4%		2.0	0.952		Berkeley (1950)
270	1σ							gg	Berkeley (1950A)

TABLE I. (*continued*).

Energy[a] (MeV)	No., type, data	Angular range (c.m.)	Data std. err.	Norm. std. err.	Deleted angles	M value[b]	Predicted norm.[c]	Comment	Reference[d]
*290	3σ	10°– 38°	20%	10%		0.0	0.991		Berkeley (1954)
*300	15σ	35°–175°	10%	10%		1.3	0.942		Berkeley (1955)
						(1.4)	(0.927)	hh	
*310	$19P$	21°–165°	20%	4%		0.8	1.004		Berkeley (1957)
						(1.1)	(1.000)	hh	
*310	$8P$	33°–142°	10%	3%		0.6	0.998		Berkeley (1967)
						(2.0)	(0.992)	hh	
310	$4D$	42°– 82°	20%					ii	Berkeley (1956)
310	$2R$	56°, 84°	45%					ii	Berkeley (1956)
*350	$1\sigma_T$		2%			0.2			Liverpool (1957)
						(0.0)		hh	
*350	17σ	114°–174°	12%	3%		0.8	1.043		Liverpool (1962)
						(0.6)	(1.008)	hh	
*350	$12P$	46°–158°	12%	Float		3.1	0.994	bb	Carnegie (1956)
						(3.7)	(1.000)	hh	
380	$1\sigma_T$		6%			0.0			Dubna (1955)
						(0.2)		hh	
380	14σ	36°–180°	12%	18%		1.6	0.954		Dubna (1954)
						(1.6)	(0.919)	hh	
*400	21σ	12°–180°	6%	3%	20°, 50°	1.4	0.993		Carnegie (1954)
						(1.2)	(0.953)	hh	
*400	$8P$	33°–144°	10%	3%		0.8	1.006		Berkeley (1967)
						(1.1)	(0.992)	hh	
*410	$1\sigma_T$		4%			0.4		jj	Chicago (1954)
500	$1\sigma_T$		6%			0.1			Dubna (1955)
500	$8P$	33°–145°	10%	3%		5.0	0.902		Berkeley (1967)
*580	17σ	35°–167°	7%	Float		3.1	0.871	kk	Dubna (1957)
*580	6σ	168°–180°	8%	Float		1.1	0.926	kk	Dubna (1957)
*580	5σ	11°– 35°	12%	Float		1.3	0.877	kk, ll	Dubna (1958)
*590	1σ	5°	15%			0.4		ll	Dubna (1959B)
*590	$1\sigma_T$		6%			0.0			Dubna (1955)
*600	$8P$	33°–146°	10%	3%		0.7	0.989		Berkeley (1967)
*600	$1\sigma_R$		7%			(16.8)		mm	Dubna (1965)
*605	$3P$	70°–125°	50%	Float		1.6	0.388	kk	Dubna (1967)
*605	$3R$	70°–125°	100%	Float		5.0	1.834	kk	Dubna (1967)
605	$1A$	125°	100%					nn	Dubna (1967)
*630	21σ	11°–180°	6%	Float		2.1	0.960	kk	Dubna (1960)
*630	$1\sigma_T$		10%			0.0			Dubna (1955)
*635	$9P$	18°–146°	20%	Float		1.6	1.010	kk	Dubna (1959A)
*635	$1D$	112.5°	80%			0.9			Dubna (1959A)
700	$8P$	29°–143°	10%	3%		2.2	1.064		Berkeley (1967)
730	$1\sigma_T$		4%			0.0			Brookhaven (1964)

[a] The starred energies are for data included in the "single-energy" analyses.
[b] These values are for the 0–400-MeV 22-parameter energy-dependent solution.
[c] This is the over-all *theoretical* normalization value arrived at in the 22-parameter search problem. The *reciprocal* of this number gives the factor by which the experimental data should be multiplied to be consistent with the phase-shift solution.
[d] The references are listed in Table II.
[e] These data were used only for the 0–400-MeV analyses.
[f] The M value and normalization values are from a preliminary solution. These data were not used in the final analyses.
[g] Some total cross sections which varied by more than one standard deviation from a theoretical curve fitted to all of the total cross sections were deleted. These were at 15.8, 19.6, 21.9, 22.4, 25.3, 26.6, 27.3, 28.0, 28.8, 30.4, 31.2, 35.1, 36.2, 37.3, 47.1, 50.6, 54.5, 61.1, 63.5, 75.3, 78.9, and 96.0 MeV.
[h] Obtained by combining four data at 16.1, 16.5, 16.8, and 17.2 MeV.
[i] Obtained by combining five data at 17.5, 17.9, 18.3, 18.7, and 19.1 MeV.
[j] Shifted in energy from 19.66 MeV.
[k] Obtained by combining four data at 20.0, 20.5, 20.9, and 21.4 MeV.
[l] These data, which were regarded by the author as preliminary, were omitted.
[m] Obtained by combining four data at 23.0, 23.5, 24.1, and 24.7 MeV.
[n] Shifted in energy from 24.0 MeV.
[o] The normalization error quoted here is from the uncertainty in the energy.
[p] Shifted in energy from 32.1 MeV.
[q] Used in the 0–400-MeV analyses, but not in the 0–750-MeV analyses.
[r] Shifted in energy from 39.75 MeV.
[s] Shifted in energy from 45.0 MeV.
[t] These data were deleted. See the discussion by Rose in reference Harwell (1966).
[u] Shifted in energy from 88.2 MeV.
[v] Shifted in energy from 91.3 MeV.
[w] Shifted in energy from 98.1 MeV.
[x] Shifted in energy from 101 MeV.
[y] Shifted in energy from 106 MeV.
[z] Shifted in energy from 111.5 MeV.
[aa] Shifted in energy from 119.6 MeV.
[bb] Normalization constant as given by Rose, reference Harwell (1966).
[cc] These data are from (p,d) measurements, with corrections as shown in the reference.
[dd] The experimental data were multiplied by the factor 1.097, as suggested by Rose, reference Harwell (1966). However, the theoretical normalization value obtained in the search suggests a preference for the unrenormalized data.
[ee] The experimental data were multiplied by the factor 0.933, as suggested by the Rose, reference Harwell (1966). However, the theoretical normalization value obtained in the search suggests a preference for the unrenormalized data.
[ff] These data contributed 91 to χ^2.
[gg] This datum was not used, but D. Measday (private communication) finds that it is reliable.
[hh] These values are for the 0–750-MeV 22-parameter energy-dependent solution.
[ii] These older data were omitted.
[jj] Above 400 MeV, all values are for the 0–750-MeV 22-parameter solution.
[kk] At the higher energies, we have treated some data sets with no constraint on the normalization. This was based partly on experience and partly on an attempt to better evaluate the consistency among the sets. We often rely on total elastic scattering cross sections to provide the correct normalization for the differential cross sections.
[ll] The data were used in the form quoted by Janout *et al.*, Dubna (1966).
[mm] Since we allowed no inelasticity for the $I=0$ amplitudes, the total (n,p) reaction cross section as calculated from the inelasticity in the (fixed) $I=1$ amplitudes was only about ⅓ of the measured value. This datum is included for comparison purposes only.
[nn] Very preliminary data, not used in the present analysis.

TABLE II. References for Table I.

Berkeley	(1949)	J. Hadley, E. Kelly, C. Leith, E. Segrè, C. Weigand, and H. York, Phys. Rev. **75**, 351 (1949).
	(1950)	E. Kelly, C. Leith, E. Segrè, and C. Wiegand, Phys. Rev. **79**, 96 (1950).
	(1950A)	J. DeJuren, Phys. Rev. **80**, 23 (1950).
	(1954)	J. W. Easley, University of California Radiation Laboratory Report No. UCRL-2693, 1954 (unpublished).
	(1955)	John DePangher, Phys. Rev. **99**, 1447 (1955).
	(1956)	D. Fischer, University of California Radiation Laboratory Report No. UCRL-3281, 1956 (unpublished).
	(1957)	O. Chamberlain, E. Segrè, R. D. Tripp, C. Wiegand, and T. Ypsilantis, Phys. Rev. **105**, 288 (1957).
	(1967)	David Cheng, Burns Macdonald, Jerome A. Helland, and Philip M. Ogden, Phys. Rev. **163**, 1470 (1967).
Brookhaven	(1952)	H. L. Poss, E. O. Salant, G. A. Snow, and L. C. L. Yuan, Phys. Rev. **87**, 11 (1952).
	(1964)	H. Palevsky, J. L. Friedes, R. J. Sutter, R. E. Chrien, and H. R. Muether, *Comptes Rendus du Congrès International de Physique Nucléaire, II*, edited by P. Gungenberger (Centre National de Recherche Scientifique, Paris, 1964), p. 162.
Canberra	(1966)	D. E. Groce and B. D. Sowerby, Nucl. Phys. **83**, 199 (1966).
Carnegie	(1954)	A. J. Hartzler, R. T. Siegel, and W. Optiz, Phys. Rev. **95**, 185 (1954); **95**, 591 (1954).
	(1956)	R. T. Siegel, A. J. Hartzler, and W. A. Love, Phys. Rev. **101**, 838 (1956).
Chicago	(1954)	V. Alexander Nedzel, Phys. Rev. **94**, 174 (1954).
Dubna	(1954)	V. P. Dzhelepov and Yu. M. Kazarinov, Dokl. Akad. Nauk SSSR **99**, 939 (1954).
	(1955)	V. P. Dzhelepov, V. I. Satarov, and B. M. Golovin, Dokl. Akad. Nauk SSSR **104**, 717 (1955).
	(1957)	Yu. M. Kazarinov and Yu. N. Simonov, Zh. Eksperim. i Teor. Fiz. **31**, 169 (1956) [English transl.: Soviet Phys.—JETP **4**, 161 (1957)].
	(1958)	N. S. Amaglobeli and Yu. M. Kazarinov, Zh. Eksperim. i Teor. Fiz. **33**, 53 (1958) [English transl.: Soviet Phys.—JETP **7**, 37 (1958)].
	(1959A)	B. M. Golovin, V. P. Dzhelepov, V. S. Nadezhdin, and V. I. Satarov, Zh. Eksperim. i Teor. Fiz. **36**, 433 (1959) [English transl.: Soviet Phys.—JETP **9**, 302 (1959)]; V. P. Dzhelepov, B. M. Golovin, V. S. Nadezhdin, and V. I. Satarov, Dubna Conference Proc. **1**, 11 (1964).
	(1959B)	B. M. Golovin, V. P. Dzhelepov, U. V. Katishev, A. D. Konin, and S. V. Medved, Zh. Eksperim. i Teor. Fiz. **36**, 735 (1959) [English transl.: Soviet Phys.—JETP **9**, 516 (1959)].
	(1960)	N. S. Amaglobeli and Yu. M. Kazarinov, Zh. Eksperim. i Teor. Fiz. **37**, 587 (1959) [English transl.: Soviet Phys.—JETP **10**, 1125 (1960)].
	(1963)	Yu. M. Kazarinov and Yu. N. Simonov, Zh. Eksperim. i Teor. Fiz. **43**, 35 (1962) [English transl.: Soviet Phys.—JETP **16**, 24 (1963)].
Dubna	(1965)	Yu. M. Kazarinov and Yu. N. Simonov, JINR Report No. P-2462, 1965 (unpublished); Yadern. Fiz. **4**, 139 (1966) [English transl.: Soviet J. Nucl. Phys. **4**, 100 (1967)].
	(1966)	Z. Janout, Yu. M. Kazarinov, F. Lehar, and A. F. Pisarev, Dubna Report No. E-2726, 1966 (unpublished); Yu. M. Kazarinov, F. Lehar, A. F. Pisarev, and Z. Janout, Yadern. Fiz. **5**, 140 (1967) [English transl.: Soviet J. Nucl. Phys. **5**, 97 (1967)].
	(1967)	Yu. M. Kazarinov, Rev. Mod. Phys. **39**, 509 (1967).
Glasgow	(1967)	W. T. Morton, Proc. Phys. Soc. (London) **91**, 899 (1967).
Haifa	(1967)	A. Suhami and R. Fox, Phys. Letters **24B**, 173 (1967).
Harvard	(1954A)	Peter Hillman, R. H. Stahl, and N. F. Ramsey, Phys. Rev. **96**, 115 (1954).
	(1954B)	R. H. Stahl and N. F. Ramsey, Phys. Rev. **96**, 1310 (1954).
	(1960)	Russell K. Hobbie and Douglas Miller, Phys. Rev. **120**, 2201 (1960).
	(1961)	A. F. Kuckes and R. Wilson, Phys. Rev. **121**, 1226 (1961); A. H. Cromer and E. H. Thorndike, *ibid.* **131**, 1680 (1963).
	(1962A)	P. M. Patel, A. Carroll, N. Strax, and D. Miller, Phys. Rev. Letters **8**, 491 (1962).
	(1962B)	R. A. Hoffman, J. Lefrançois, E. H. Thorndike, and Richard Wilson, Phys. Rev. **125**, 973 (1962); J. Lefrançois, R. A. Hoffman, E. H. Thorndike, and Richard Wilson, *ibid.* **131**, 1660 (1963); A. H. Cromer and E. H. Thorndike, *ibid.* **131**, 1680 (1963).
	(1964A)	W. G. Collins, Jr., and D. G. Miller, Phys. Rev. **134**, B575 (1964).
	(1964B)	A. S. Carroll, P. M. Patel, N. Strax, and D. Miller, Phys. Rev. **134**, B595 (1964).
	(1966A)	D. F. Measday and J. N. Palmieri, Nucl. Phys. **85**, 142 (1966).
	(1966B)	David F. Measday, Phys. Rev. **142**, 584 (1966).
	(1967)	N. Strax (unpublished); R. Wilson (private communication).
Harwell	(1952A)	T. C. Randle, A. E. Taylor, and E. Wood, Proc. Roy. Soc. (London) **A213**, 392 (1952).
	(1952B)	A. E. Taylor and E. Wood, Phil. Mag. **44**, 95 (1952).
	(1956)	T. C. Randle, D. M. Skyrme, M. Snowden, A. E. Taylor, F. Uridge, and E. Wood, Proc. Phys. Soc. (London) **A69**, 760 (1956).
	(1957)	G. H. Stafford, C. Whitehead, and P. Hillman, Nuovo Cimento **5**, 1589 (1957).
	(1960)	C. Whitehead, S. Tornabene, and G. H. Stafford, Proc. Phys. Soc. (London) **75**, 345 (1960).
	(1961)	P. H. Bowen, J. P. Scanlon, G. H. Stafford, J. J. Thresher, and P. E. Hodgson, Nucl. Phys. **22**, 640 (1961).
	(1963)	J. P. Scanlon, G. H. Stafford, J. J. Thresher, P. H. Bowen, and A. Langsford, Nucl. Phys. **41**, 401 (1963).
	(1965)	A. Langsford, P. H. Bowen, G. C. Cox, G. B. Huxtable, and R. A. J. Riddle, Nucl. Phys. **74**, 241 (1965).
	(1966)	B. Rose, Phys. Letters **20**, 86 (1966).
Livermore	(1958)	A. Bratenahl, J. M. Peterson, and J. P. Stoering, Phys. Rev. **110**, 927 (1958).

TABLE II. (*continued*).

Livermore	(1960)	J. M. Peterson, A. Bratenahl, and J. P. Stoering, Phys. Rev. **120**, 521 (1960).
Liverpool	(1957)	A. Ashmore, R. G. Jarvis, D. S. Mather, and S. K. Sen, Proc. Phys. Soc. (London) **A70**, 745 (1957).
	(1962)	A. Ashmore, W. H. Range, R. T. Taylor, B. M. Townes, L. Castillejo, and R. F. Peierls, Nucl. Phys. **36**, 258 (1962).
Los Alamos	(1953)	J. C. Allred, A. H. Armstrong, and L. Rosen, Phys. Rev. **91**, 90 (1953).
	(1955A)	J. D. Seagrave, Phys. Rev. **97**, 757 (1955).
	(1955B)	R. B. Day, R. L. Mills, J. E. Perry, Jr., and F. Scherb, Phys. Rev. **98**, 279 (1955).
	(1962)	E. R. Flynn and P. J. Bendt, Phys. Rev. **128**, 1268 (1962).
	(1963)	R. B. Perkins and J. E. Simmons, Phys. Rev. **130**, 272 (1963).
	(1964)	R. B. Perkins and J. E. Simmons, *Comptes Rendus du Congrès International de Physique Nucléaire, II*, edited by P. Gungenberger (Centre National de Recherche Scientifiques, Paris, 1964), Vol. II, p. 164; and (private communication).
	(1966)	J. J. Malanify, P. J. Bendt, T. R. Roberts, and J. E. Simmons, Phys. Rev. Letters **17**, 481 (1966); and (private communication from the authors).
Oxford	(1955)	J. J. Trehsher, R. G. P. Voss, and R. Wilson, Proc. Roy. Soc. (London) **A229**, 492 (1955).
Rochester	(1952)	George R. Mott, Gordon L. Guernsey, and Bruce K. Nelson, Phys. Rev. **88**, 9 (1952).
	(1961)	John H. Tinlot and Robert E. Warner, Phys. Rev. **124**, 890 (1961); and Rochester (1967C).
	(1962)	Robert E. Warner and John H. Tinlot, Phys. Rev. **125**, 1028 (1962); and Rochester (1967C).
	(1966)	N. W. Reay, E. H. Thorndike, D. Spalding, and A. R. Thomas, Phys. Rev. **150**, 801 (1966); and Rochester (1967C).
	(1967A)	D. Spalding, A. R. Thomas, and E. H. Thorndike, Phys. Rev. **158**, 1338 (1967).
	(1967B)	A. R. Thomas, D. Spalding, and E. H. Thorndike, Phys. Rev. **167**, 1240 (1968); and Rochester (1967C).
	(1967C)	Edward H. Thorndike, Rev. Mod. Phys. **39**, 513 (1967).
Rutherford	(1962)	G. H. Stafford and C. Whitehead, Proc. Phys. Soc. (London) **79**, 430 (1962).
Wisconsin	(1962)	W. Benenson, R. L. Walter, and T. H. May, Phys. Rev. Letters **8**, 66 (1962).

BSSTH measurements were combined, with energy shifting and statistical weighting, into four averaged data points. Thus our final data selected included 24 BSSTH total-cross-section measurements treated directly, 17 more treated as averaged data, and 28 measurements by other groups, in the energy range below 130 MeV. These details are all given in Table I.

One result of the analysis, as can be seen from the M values (M is the average contribution to χ^2 per datum) quoted in Table I, is that several other total-cross-section measurements[6] are in disagreement with the BSSTH measurements by about 2% at the low energies and 3–4% at the higher energies. The BSSTH values are lower. This discrepancy is larger than the quoted uncertainties in the measurements. Most of the BSSTH data that we excluded were even lower than those used, so that if we had retained the entire set of BSSTH data, the discrepancy with the values obtained by the other workers[6] would have been even greater.

Since our phase-shift solutions from the (n,p) analysis are largely qualitative, it is difficult to make many statements, based on the analyses, as to the accuracy of the data. The polarization data from 126 to 143 MeV were given the renormalizations and normalization errors suggested by Rose.[7] In particular, polarization measurements at 140 and 143 MeV, which were formerly in general agreement, were renormalized 10% upward and 9% downward, respectively. However, in the computer search calculation, the theoretical normalizations readjusted to cancel out the effect of the renormalization. (Rose had also suggested that the 143-MeV polarization data should be deleted.)

The data from 300 to 400 MeV are shown with the M values and renormalization assignments as given by both the 0–400- and the 0–750-MeV analyses. As can be seen, the two types of analysis give very similar results. This indicates that form-limiting effects (constraints imposed by the phase-shift energy-dependent forms) are quite small, at least in this energy region.

In the energy region above 400 MeV, the results we have obtained are so sketchy that it is difficult to draw any conclusions from our work as to the consistency of the data. However, even though we have solution ambiguities above 400 MeV, the existing data do impose constraints on the amplitudes and do help to sharpen our knowledge of the phases in the energy region just below 400 MeV. The importance of this is discussed in Sec. VI, in which we compare the present results with the recent Yale (Y-IV) $pp+np$ solution.

III. SINGLE-ENERGY ANALYSES BELOW 400 MeV

In a systematic phase-shift analysis program, we first carry out energy-dependent analyses. Then, using the phase-shift energy derivatives thus obtained at certain selected energies, and using the information we have gained about the data compatibility, we carry out a set of energy-independent analyses. This procedure was followed in the present work. However, in order to

[6] These are the references Livermore (1958), Brookhaven (1952), Canberra (1966), Los Alamos (1955B), and Harvard (1966A) of Table II.

[7] B. Rose, Phys. Letters **20**, 86 (1966).

TABLE III. Summary of combined (p,p) plus (n,p) single-energy phase-shift analyses. The (p,p) data were represented by matrices from the single-energy solutions of Tables VI and VII in Paper VII. The (n,p) data were treated directly. The isotopic spin $I=1$ phases were first held fixed at the values from Table VI of Paper VII, with the $I=0$ phases being searched. Then both the $I=1$ and $I=0$ phases were searched together.

Energy (MeV)	No. of data (p,p)[a]	No. of data (n,p)	Energy spread (MeV)[b]	No. of phases $I=1$	No. of phases $I=0$	χ^2 $I=1$ fixed	χ^2 Both searched[c]
25	34	71	20.5–30	5	4	56.7	56.4*
25				5	6	55.7	55.5
50	99	103	47.5–60	9	4	234.0	220.2
50				9	6	181.1	180.1*
50				9	8	178.6	177.4
95	85	124	89.5–100	9	6	204.2	201.5*
95				9	8	201.0	198.4
142	183	118	128 –153	11	8	309.6	309.1*
142				11	11	300.4	300.0
210	65	56	197 –215	14	8	85.6	85.4*
210				14	11	84.2	83.9
330	122	75	290 –350	14	8	211.7	200.9
330				14	11	187.6	186.9*
330				14	13	186.8	186.1

[a] Represented by a matrix.
[b] (n,p) data only.
[c] The starred solutions are favored.

justify the way in which we handled the energy-dependent analysis, we must first discuss the energy-independent results.

The difficulty in carrying out (n,p) analyses is that the (n,p) scattering experiments are not complete enough to permit an analysis using only (n,p) data. We attempted such an analysis at 140 MeV, as described in Paper I, and found essentially an infinity of solutions. Thus the (n,p) data must be combined with information about the isovector ($I=1$) scattering amplitudes as obtained from (p,p) scattering. Some assumption about charge independence must be invoked if one is to do any kind of meaningful analysis of the isoscalar ($I=0$) scattering amplitudes.

In Papers I–VI, we have described many studies which show comparisons of analyses using first (p,p) data, and then (p,p) plus (n,p) data. The conclusion that was repeatedly obtained in these studies was that the $I=1$ scattering amplitudes are essentially fixed by the (p,p) scattering data. Little information is obtained about the $I=1$ amplitudes by analyzing the existing (n,p) data. However, if we believe the statement of charge independence, that the $I=1$ nuclear amplitudes are essentially the same for (p,p) as for (n,p) scattering, then the (n,p) data when analyzed in conjunction with the (p,p) data can supply considerable information about the $I=0$ amplitudes.

To reverify these remarks, we carried out the set of single-energy studies shown in Table III. Our starting point was the single-energy (p,p) solutions listed in Table VI of Paper VII. Matrix representations of the (p,p) data sets used in obtaining these solutions were combined with the available (n,p) data in the same energy bands, as shown in Table III and in Table I. Search problems were carried out first by holding the $I=1$ phases fixed at the (p,p) values and searching only the $I=0$ phases, and second by searching both the $I=1$ and $I=0$ phases. As the last two columns of Table III show, the χ^2 values for these two procedures are almost identical provided that a sufficient number of $I=0$ phases are included in the search. This confirms the fact that the existing (n,p) data are consistent with the (p,p) $I=1$ scattering amplitudes.

The starred solutions in Table III are the ones that seem to us to be most physically significant. The phases for these solutions are given in Table IV. As can be seen in Table IV, the changes produced in the $I=1$ phases when they are released in the combined (p,p) plus (n,p) search problem are much smaller than the uncertainties in these phases. This is of course what we expect from the χ^2 values listed in Table III. When the $I=1$ phases are included in the search, the experimental uncertainties in these phases *decrease* from the values that were obtained by using only (p,p) data. This is expected, since a larger data selection is being fit. Releasing the $I=1$ phases *increases* the uncertainties in the $I=0$ phases, as shown in Table IV, which is again the expected result. However, the point that we wish to emphasize here is that the increase in the $I=0$ phase-shift uncertainties when the $I=1$ phases are freed is in general a small one, as shown in Table IV. The experimental uncertainties in the $I=0$ amplitudes come largely from the incompleteness of the (n,p) data selection, and not from any lack of knowledge about the $I=1$ amplitudes. In the energy-independent analyses, we have obtained solutions both with the $I=1$ phases fixed at the (p,p) values, and with the $I=1$ phases searched. However, in the energy-dependent analyses to be described in Sec. IV, we held the $I=1$ amplitudes fixed and searched only the $I=0$ amplitudes. In the analyses described in Paper IV, we carried out energy-dependent analyses in which both the $I=1$ and $I=0$ amplitudes were searched simultaneously. But this refinement in the analysis adds nothing in a practical sense to the accuracy with which we can at present determine the $I=0$ amplitudes.

Figure 1 shows the $I=0$ phases from the single-energy analyses plotted together with the energy-dependent solution described in Sec. IV. The agreement between the two types of analysis is good, although it is qualitative and is not as favorable as for the $I=1$ phases shown in Fig. 1 of Paper VII. The lack of more exact quantitative agreement indicates, in our opinion, inadequacies in the (n,p) data.

If we believe, as we have tried to demonstrate here, that the charge-independence assumption is a good one, then the six solutions of Table IV in which the $I=1$ and $I=0$ phases were both searched represent the best over-all single-energy determinations of the $I=1$ and $I=0$ amplitudes we can obtain with the existing elastic nucleon-nucleon data. Accordingly, we give in Tables V–XII the second-derivative matrices and the error

TABLE IV. Single-energy (p,p) plus (n,p) phase-shift solutions. The phases in parentheses were held fixed at values obtained by fitting just (p,p) data (Table VI of Paper VII). The solutions with $I=1$ and $I=0$ both searched correspond to the starred solutions in Table III. Second-derivative matrices and error matrices for these starred solutions are given in Tables V–XII.

$T=1$	25 MeV		50 MeV		95 MeV		142 MeV		210 MeV		330 MeV	
No. of data	Fixed 105	Searched 105	Fixed 202	Searched 202	Fixed 209	Searched 209	Fixed 301	Searched 301	Fixed 116	Searched 116	Fixed 197	Searched 197
χ^2	56.7	56.4	181.1	180.1	204.2	201.5	309.6	309.1	85.6	85.4	187.6	186.9
$^1S_0$	(48.61±0.26)	48.60±0.26	(39.55±0.46)	39.52±0.44	(26.87±1.44)	26.22±1.26	(16.50±0.58)	16.65±0.55	(5.59±0.53)	5.53±0.52	(−10.70±1.46)	−10.94±1.40
$^1D_2$	(0.76±0.03)	0.76±0.03	(1.74±0.10)	1.75±0.09	(3.77±0.26)	3.59±0.20	(4.95±0.17)	4.99±0.17	(7.03±0.29)	7.04±0.27	(9.09±0.52)	9.03±0.48
$^1G_4$							(0.81±0.07)	0.79±0.06	(1.10±0.10)	1.10±0.10	(1.20±0.25)	1.30±0.24
$^3P_0$	(8.53±0.45)	8.46±0.31	(10.78±0.69)	11.08±0.60	(11.17±2.15)	11.21±1.68	(5.74±0.54)	5.87±0.49	(−1.23±0.55)	−1.13±0.54	(−12.40±1.57)	−12.24±1.55
$^3P_1$	(−5.01±0.21)	−5.06±0.16	(−8.16±0.31)	−8.06±0.23	(−13.12±0.66)	−12.88±0.44	(−17.07±0.17)	−17.07±0.16	(−22.20±0.32)	−22.16±0.31	(−28.36±1.20)	−27.85±1.16
$^3P_2$	(2.43±0.16)	2.47±0.08	(5.70±0.15)	5.74±0.14	(9.70±0.50)	9.96±0.40	(13.73±0.11)	13.71±0.11	(15.59±0.23)	15.65±0.22	(16.18±0.56)	16.16±0.55
ϵ_2			(−1.74±0.21)	−1.73±0.19	(−2.72±0.32)	−2.55±0.29	(−2.85±0.07)	−2.85±0.07	(−2.86±0.16)	−2.85±0.15	(−2.54±0.44)	−2.63±0.41
$^3F_2$			(−0.15±0.29)	−0.07±0.26	(−0.19±0.92)	0.29±0.47	(0.84±0.27)	0.72±0.23	(1.33±0.31)	1.22±0.29	(0.42±0.57)	0.22±0.55
$^3F_3$			(−0.39±0.39)	−0.46±0.37	(−0.62±0.92)	−0.59±0.72	(−2.13±0.17)	−2.05±0.16	(−2.63±0.20)	−2.66±0.20	(−3.54±0.61)	−3.62±0.59
$^3F_4$			(0.17±0.18)	0.11±0.13	(0.40±0.28)	0.51±0.16	(0.98±0.14)	0.93±0.12	(2.09±0.18)	2.02±0.18	(2.80±0.24)	2.75±0.22
ϵ_4							(−0.77±0.03)	−0.77±0.03	(−1.02±0.09)	−1.01±0.09	(−0.99±0.29)	−0.89±0.22
$^3H_4$									(0.10±0.23)	0.15±0.19	(1.23±0.34)	1.32±0.27
$^3H_5$									(−1.00±0.20)	−0.98±0.17	(−1.92±0.52)	−1.91±0.48
$^3H_6$									(0.07±0.14)	0.10±0.12	(0.67±0.16)	0.74±0.14
$^1P_1$	−4.29±1.36	−4.15±1.38	−0.65±1.08	−0.74±1.16	−10.28±1.02	−12.93±2.20	−17.57±1.29	−17.40±1.34	−21.29±1.68	−21.27±1.87	−41.03±1.76	−41.14±1.96
$^1F_3$							−2.63±0.47	−2.62±0.48	−4.24±0.70	−4.30±0.87	−3.80±0.60	−3.76±0.75
$^3S_1$	85.31±1.59	85.42±1.64	64.08±1.76	63.18±1.86	44.90±1.30	45.43±1.58	30.11±0.60	30.00±0.63	14.20±1.31	14.16±1.34	8.46±1.79	8.81±2.15
ϵ_1	−0.39±1.10	−0.50±1.12	−0.05±2.64	1.62±2.98	−0.03±1.56	−0.12±1.72	3.50±0.65	3.45±0.68	6.20±0.70	6.20±0.71	7.99±2.30	7.24±2.63
$^3D_1$	−3.27±0.16	−3.32±0.18	−5.14±1.60	−6.02±1.72	−11.75±0.59	−11.49±0.87	−15.11±0.50	−15.06±0.51	−18.14±1.39	−18.10±1.44	−30.19±1.58	−30.45±1.82
$^3D_2$			9.15±1.74	10.19±1.85	15.91±1.54	14.37±2.27	22.56±0.74	22.74±0.80	28.06±1.00	28.07±1.02	16.89±1.81	17.27±2.18
$^3D_3$			1.74±0.88	1.21±0.96	1.80±0.54	1.90±0.71	2.07±0.44	2.05±0.45	4.32±0.75	4.25±0.82	2.99±1.15	2.98±1.21
ϵ_3							4.57±0.30	4.60±0.31	6.44±0.30	6.49±0.36	9.84±0.45	9.87±0.60
$^3G_3$											−4.04±1.58	−3.72±1.70
$^3G_4$											1.47±1.32	1.41±1.46
$^3G_5$											−0.82±0.66	−0.78±0.67

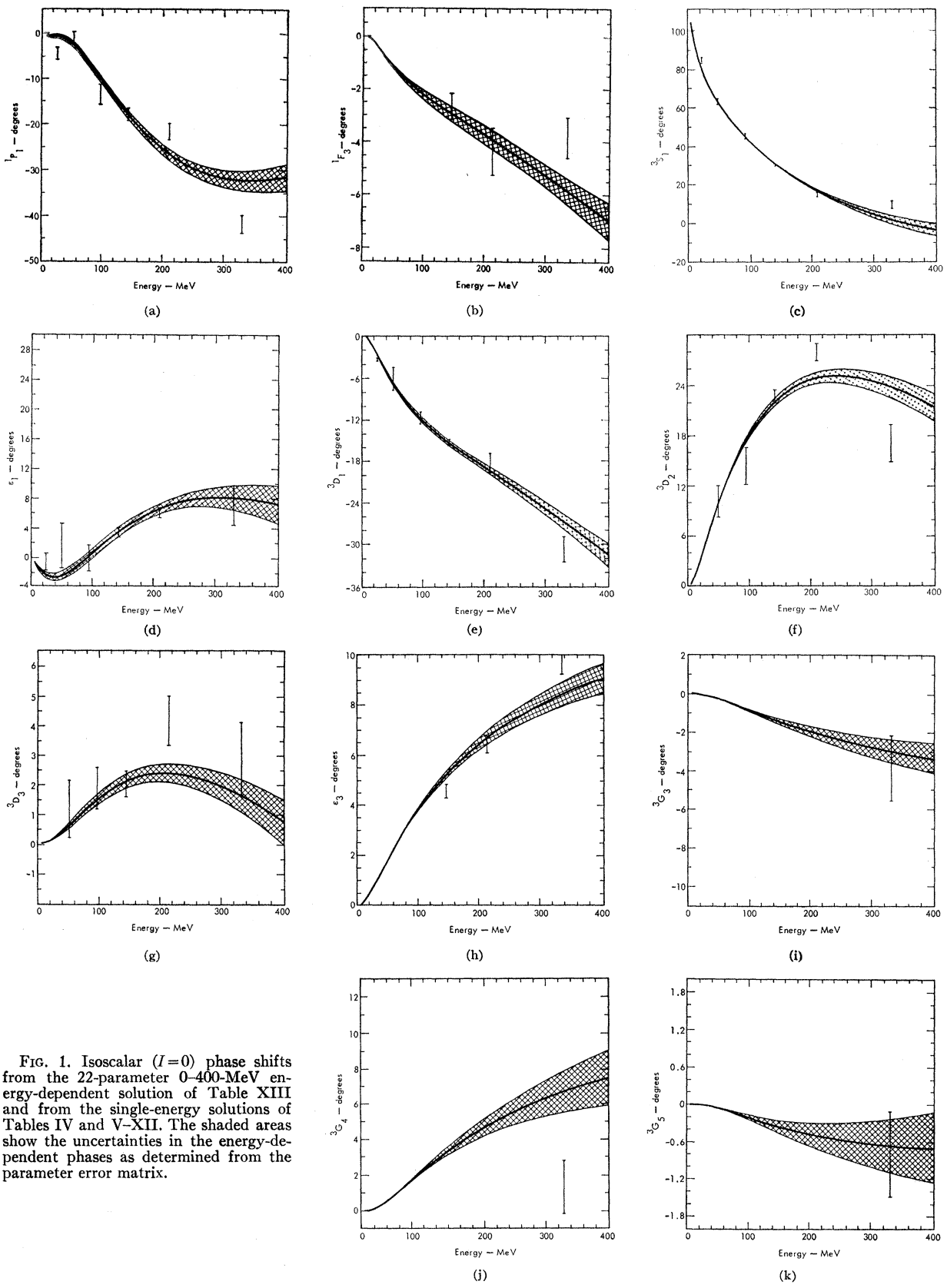

FIG. 1. Isoscalar ($I=0$) phase shifts from the 22-parameter 0–400-MeV energy-dependent solution of Table XIII and from the single-energy solutions of Tables IV and V–XII. The shaded areas show the uncertainties in the energy-dependent phases as determined from the parameter error matrix.

matrices for these six solutions. Also given are the matrices for the 425-MeV single-energy analysis, which is discussed in Sec. V, and the $I=1$ and $I=0$ phase-shift values that correspond to all of the matrices. As we have discussed in Paper VII, the second-derivative matrix can be used instead of the actual data selection in minimizing χ^2 for the predictions of any particular model. For almost all purposes, we have verified that the use of the second-derivative matrix is fully as accurate as making a direct fit to the data, and, from a computational standpoint, fitting to the matrix is vastly simpler and quicker. The error matrix can be used to obtain the experimental uncertainties in any desired observable at that energy. The equations for the uses of

TABLE V. Second-derivative matrix (below the diagonal, in deg^{-2}) and error matrix (above the diagonal, in deg^2) for the 25-MeV solution of Table IV (both $I=0$ and $I=1$ phases included in the search).

	$^1P_1$	$^3S_1$	ϵ_1	$^3D_1$	$^1S_0$	$^3P_0$	$^3P_1$	$^1D_2$	$^3P_2$	
	0.19096+1	0.12073+1	−0.14592+1	−0.38156−1	0.79684−2	−0.39345−1	−0.18968−1	0.16934−2	0.17043−1	$^1P_1$
		0.26914+1	−0.10421+1	−0.10586−1	−0.75104−1	−0.45526−1	−0.30343−2	0.49611−2	0.15211−1	$^3S_1$
$^1P_1$	0.46223+1		0.12627+1	0.35316−1	0.69598−2	0.34465−1	0.19341−1	−0.83549−3	−0.15991−1	ϵ_1
$^3S_1$	−0.58222−1	0.59096		0.33128−1	0.15598−2	0.15864−1	0.65467−2	−0.36960−3	−0.64348−2	$^3D_1$
ϵ_1	0.53144+1	0.42569	0.73526+1		0.65787−1	−0.28147−1	0.14397−1	−0.27546−2	−0.55634−2	$^1S_0$
D_1	−0.13444	−0.44598	−0.10322+1	0.40643+2		0.97732−1	−0.19750−1	0.44084−3	−0.63931−2	$^3P_0$
$^1S_0$	−0.16779+1	0.87991	−0.12311+1	−0.49885	0.23492+2		0.24055−1	0.13922−4	−0.64206−2	$^3P_1$
$^3P_0$	−0.43338	0.37027	−0.49124	−0.76897+1	0.68146+1	0.24784+2		0.10820−2	0.91901−3	$^1D_2$
$^3P_1$	0.10996	−0.36054	−0.77241	−0.11332+2	−0.47220+1	0.34623+2	0.11645+3		0.67454−2	$^3P_2$
$^1D_2$	−0.71854+1	−0.52019	−0.87457+1	0.11943+1	0.42298+2	−0.48555+2	−0.15724+3	0.13545+4		
$^3P_2$	0.21149	0.20246	0.10331+1	0.19021+2	0.14437+2	0.60441+2	0.14908+3	−0.34561+3	0.42604+3	

TABLE VI. Second-derivative matrix (below the diagonal, in deg^{-2}) and error matrix (above the

	$^1P_1$	$^3S_1$	ϵ_1	$^3D_1$	$^3D_2$	$^3D_3$	$^1S_0$	$^3P_0$
	0.13564+1	−0.65268	−0.93379	−0.77121	0.69953	−0.38652	0.64565−1	−0.20242
		0.34466+1	−0.28906+1	0.28798+1	−0.31642+1	0.15949+1	−0.62327−2	−0.56303−1
$^1P_1$	0.12751+1		0.88914+1	−0.20900+1	0.28402+1	−0.11682+1	−0.75818−1	0.56702
$^3S_1$	0.20057	0.20271+1		0.29714+1	−0.31152+1	0.16320+1	−0.31824−1	0.40170−1
ϵ_1	0.28455	0.18779	0.31287		0.34373+1	−0.17132+1	0.24324−1	0.35173−1
$^3D_1$	0.11646+1	0.48667	0.22143	0.33916+2		0.92190	−0.10620−1	−0.14954−1
$^3D_2$	−0.70746−1	0.12896+1	−0.52605	0.11525+2	0.10319+2		0.19150	−0.19414
$^3D_3$	−0.16124+1	−0.16971+1	−0.11800+1	−0.39203+2	−0.42263+1	0.64474+2		0.35412
$^1S_0$	0.38663−1	0.72575	−0.54998−2	−0.44607	0.51398	0.45739	0.18741+3	
$^3P_0$	0.35596	0.18963	−0.25324	−0.53134+1	−0.10867+1	0.68309+1	0.43479+2	0.72950+2
$^3P_1$	0.49687	−0.10226+1	−0.79174	−0.11294+2	−0.28570+1	0.15581+2	−0.18476+3	0.58066+2
$^1D_2$	−0.80104	−0.25842	−0.58728	0.19955+1	0.53754+1	0.63852+1	0.56515+3	−0.36912+3
$^3P_2$	0.28341+1	0.18871+1	0.15329+1	0.18799+2	0.69927+1	−0.20149+2	0.14339+2	0.32459+3
ϵ_2	−0.84106	−0.94804	−0.30902	0.27707+1	0.28217+1	0.20392+1	0.25688+3	−0.27177+3
$^3F_2$	0.77647	−0.77501	−0.77184	−0.16868+2	−0.28084+1	0.28244+2	−0.54672+2	0.12623+3
$^3F_3$	0.20582+1	0.10583	0.96655−1	−0.44385+1	−0.37571	0.88747+1	−0.23139+3	0.34393+3
$^3F_4$	0.19475+1	0.17864+1	0.55966	0.20572+2	0.74436+1	−0.29069+2	0.58862+2	0.30169+3

TABLE VII. Second-derivative matrix (below the diagonal, in deg^{-2}) and error matrix (above the diagonal,

	$^1P_1$	$^3S_1$	ϵ_1	$^3D_1$	$^3D_2$	$^3D_3$	$^1S_0$	$^3P_0$
	0.48586+1	−0.11083+1	0.84512	−0.72639	0.34979+1	−0.31793	0.21009	−0.85993
		0.25089+1	−0.21078+1	0.10759+1	−0.29086+1	0.86755	−0.54327	0.95479
$^1P_1$	0.47199+1		0.29588+1	−0.88116	0.27866+1	−0.70683	−0.10796	−0.78311
$^3S_1$	0.64897	0.43090+1		0.75698	−0.16516+1	0.51817	−0.12109	0.93077
ϵ_1	0.26735+1	0.15650+1	0.34036+1		0.51590+1	−0.12551+1	0.20495	−0.17435+1
$^3D_1$	−0.26325+1	−0.15593+1	−0.20425+1	0.11196+2		0.50133	−0.22318−1	0.51490
$^3D_2$	−0.64734+1	0.31274	−0.46314+1	0.48848+1	0.11829+2		0.15878+1	−0.17735
$^3D_3$	−0.84826+1	−0.32226+1	−0.50360+1	0.46591	0.13051+2	0.29442+2		0.28377+1
$^1S_0$	−0.48916	0.67502	−0.57596−1	−0.30967	0.67586	0.19608	0.64765+1	
$^3P_0$	0.61701	0.71678	0.23889	−0.13920+1	−0.20404	−0.46584	−0.98957	0.17774+1
$^3P_1$	−0.16879	−0.17961+1	−0.37805	−0.15490+1	0.37604	0.54630+1	0.11827+2	−0.25905+1
$^1D_2$	−0.93586+1	−0.36709+1	−0.46799+1	0.65853+1	0.10817+2	0.18373+2	0.26892+2	0.16855+1
$^3P_2$	0.48644+1	0.58325+1	0.48224+1	−0.11618+1	−0.36737+1	−0.76919+1	−0.16911+2	0.62029+1
ϵ_2	−0.54109+1	−0.31357+1	−0.33391+1	0.57233+1	0.66156+1	0.13827+2	0.17914+2	0.92585+1
$^3F_2$	0.21037+1	0.89012	−0.11779+1	−0.27859+1	0.48407	−0.13285+1	0.15688+2	−0.53879+1
$^3F_3$	0.53687+1	0.30940+1	0.30827+1	−0.31485+1	−0.41478+1	−0.69612+1	−0.91099+1	−0.13292+1
$^3F_4$	0.19193+1	0.11345+1	−0.36822+1	0.14164+1	0.42146+1	−0.67066+1	−0.15399+1	0.93977+1

these matrices are given in the Appendix. As we have shown in Table IX of Paper VII, the data included in these "single-energy" bands contain most of the physical content of the data over the entire elastic scattering range. Thus a potential modelist who fits to the second-derivative matrices of Tables V–XII will obtain parameters that give a precision fit to the entire body of nucleon-nucleon elastic scattering data.

It should perhaps be noted that in regions where the data are not sufficient to define a solution accurately, such as is the case at present for (n,p) scattering below 50 MeV and above roughly 300 MeV, this same uncertainty will carry over into the second-derivative matrices. Using the second-derivative matrices (and sometimes using the data directly) can give misleading results in these regions.

IV. ENERGY-DEPENDENT ANALYSIS BELOW 400 MeV

In Paper IV, we described an energy-dependent analysis in which first (p,p) data and then (p,p) plus (n,p) data were used to obtain phase-shift solutions. The $I=1$ phases for these two types of analysis were very similar, as shown in Fig. 1 of Paper IV. As described in Sec. III of the present paper, this same conclusion about the validity of the charge-independence hypothesis holds with our expanded data set. Accordingly, we made energy-dependent analyses for the present paper in which the $I=1$ phases were fixed at the values obtained from fits to (p,p) data (Paper VII), and the $I=0$ phases were varied to minimize χ^2 in searches using just (n,p) data. Since the (n,p) data are still woefully incomplete, the $I=0$ amplitudes as determined in any kind of analysis have large uncertainties, and these uncertainties are large compared to changes produced by a different treatment of the $I=1$ amplitudes. Expressed somewhat differently, it is our calculational experience that the error matrix for the combined (p,p) plus (n,p) elastic phase-shift solution can be expressed as accurately as the data allow by the direct product of an $I=1$ error matrix with an $I=0$ error matrix. In an historical context, we believe that

diagonal, in deg²) for the 50-MeV solution of Table IV (both $I=0$ and $I=1$ phases included in the search).

$^3P_1$	$^1D_2$	$^3P_2$	ϵ_2	$^3F_2$	$^3F_3$	$^3F_4$	
−0.59072−1	−0.15853−1	−0.12599−1	0.51115−1	−0.38745−1	0.88792−1	0.19166−2	$^1P_2$
−0.12463−1	0.14552−2	−0.25175−1	−0.40606−1	−0.18052−2	−0.34586−1	0.48768−1	$^3S_1$
0.18737	0.12764−1	0.11860−1	−0.64229−1	0.11722	−0.18458	−0.45621−1	ϵ_1
0.13709−1	0.49040−2	−0.24587−1	−0.64212−1	0.23776−1	−0.82693−1	0.52672−1	$^3D_1$
0.11704−1	−0.40822−2	0.23148−1	0.55071−1	−0.85591−2	0.57540−1	−0.56715−1	$^3D_2$
−0.38602−2	0.84837−3	−0.16267−1	−0.31765−1	0.72580−2	−0.35815−1	0.33779−1	$^3D_3$
0.34777−1	−0.14761−1	−0.40025−1	0.57960−1	−0.81769−1	0.12653	−0.20533−1	$^1S_0$
0.22092−1	0.22190−1	0.39056−1	−0.70720−1	0.85097−1	−0.15043	0.64368−3	$^3P_0$
0.51738−1	0.77606−2	0.24693−2	−0.88191−2	−0.15571−1	0.23602−3	−0.14566−1	$^3P_1$
	0.78716−2	0.73661−2	−0.10369−1	−0.34104−2	−0.60339−2	−0.39801−2	$^1D_2$
0.50316+3		0.19111−1	−0.14975−1	0.13961−1	−0.28456−1	−0.25306−2	$^3P_2$
−0.42090+3	0.16358+5		0.35049−1	−0.27815−1	0.57701−1	−0.90025−2	ϵ_2
0.51034+3	−0.34585+4	0.20607+4		0.68695−1	−0.87126−1	0.20907−1	$^3F_2$
−0.87472+2	0.11376+5	−0.23489+4	0.83189+4		0.13576	−0.25686−1	$^3F_3$
0.32570+3	−0.15993+4	0.81770+3	−0.12648+4	0.67192+3		0.15772−1	$^3F_4$
0.74024+3	−0.63889+4	0.24285+4	−0.45330+4	0.13573+4	0.38034+4		
0.91618+3	0.21423+4	0.14686+4	0.18000+4	0.53573+3	0.94743+3	0.36264+4	

in deg²) for the 95-MeV solution of Table VI (both $I=0$ and $I=1$ phases included in the search).

$^3P_1$	$^1D_2$	$^3P_2$	ϵ_2	$^3F_2$	$^3F_3$	$^3F_4$	
−0.27985	0.20115	−0.22237	−0.16411	−0.45765	−0.25820	−0.22226	$^1P_1$
0.11419	0.15102−1	−0.12792	−0.73339−1	0.90122−1	−0.35211−1	0.68563−1	$^3S_1$
−0.15589	−0.41447−1	0.20649−1	0.39846−1	0.71185−1	−0.15139	−0.72747−2	ϵ_1
0.19560−1	−0.49583−2	−0.30772−2	−0.85516−1	0.13180	−0.13326	0.50467−1	$^3D_1$
−0.12145	0.80250−1	−0.81578−1	0.57438−1	−0.39248	0.26529−1	−0.19403	$^3D_2$
−0.67142−1	−0.20758−2	−0.12679−1	−0.66864−1	0.10185	−0.11935	0.44910−1	$^3D_3$
−0.22563	−0.52244−1	−0.15132−1	0.98559−1	−0.24217	0.36580	−0.10505−1	$^1S_0$
0.13274	0.54374−1	0.12491−1	−0.27378	0.16897	−0.40154	0.85244−2	$^3P_0$
0.18948	0.54744−3	0.20656−1	0.11367−1	−0.17309−1	0.42855−1	−0.14865−1	$^3P_1$
	0.41829−1	−0.38223−2	−0.35654−1	−0.23442−1	−0.23118−1	−0.14596−1	$^1D_2$
0.33393+2		0.15959	−0.34785−1	0.12175	−0.15548	0.14599−3	$^3P_2$
0.52488+2	0.28197+3		0.83440−1	−0.46995−1	0.16431	0.93595−2	ϵ_2
−0.35670+2	−0.65645+2	0.81535+2		0.21847	−0.23140	0.37849−1	$^3F_2$
0.34823+2	0.27276+3	−0.24840+2	0.35328+3		0.51871	0.10278−1	$^3F_3$
0.27920+2	0.11616+2	−0.68187+2	−0.47255+2	0.12400+3		0.24674−1	$^3F_4$
−0.19688+2	−0.11318+3	0.19951+2	−0.13931+3	0.35041+2	0.72943+2		
0.90128+1	0.98212+2	0.52079+2	0.15755+3	−0.12619+3	−0.86477+2	0.32518+3	

TABLE VIII. Second-derivative matrix (below the diagonal, in deg^{-2}) and error matrix (above the diagonal,

	$^1P_1$	$^3S_1$	ϵ_1	$^3D_1$	$^3D_2$	$^3D_3$	$^1F_3$	ϵ_3	$^1S_0$	$^3P_0$
	0.18055+1	0.17093	−0.40276	0.37800−1	0.66643	0.14782	−0.25333	0.51572−1	0.39931−1	0.46303−1
		0.40162	−0.19025	−0.21393	−0.17337	−0.20942−1	−0.73699−1	−0.13884−1	−0.83791−1	−0.56805−1
$^1P_1$	0.49892+1		0.45895	0.17282	−0.65261−1	0.11620	0.64617−1	0.39437−1	−0.24731−1	−0.45439−1
$^3S_1$	−0.17632+1	0.66831+1		0.26328	0.23801	0.94507−1	0.10840	−0.22638−1	0.51035−1	0.44025−1
ϵ_1	0.45752+1	−0.16176	0.10601+2		0.64695	0.87791−1	0.48292−1	−0.42756−1	0.97846−1	0.82718−1
$^3D_1$	−0.28537+1	0.49411+1	−0.80732+1	0.19369+2		0.20035	0.82678−1	0.12247−2	−0.38904−2	−0.18440−1
$^3D_2$	−0.33718+1	0.19014+1	−0.72398	−0.31898+1	0.71516+1		0.23499	−0.90335−1	0.23864−1	0.12764−1
$^3D_3$	−0.75257+1	−0.55868	−0.81713+1	0.22314+1	0.21126+1	0.23076+2		0.97889−1	0.18460−1	0.25145−1
$^1F_3$	0.88740+1	−0.11709+1	0.76476+1	−0.72849+1	−0.23896+1	−0.20625+2	0.30498+2		0.30570	0.10845
ϵ_3	0.18392+1	0.24621+1	−0.24867+1	0.20208+1	0.32738+1	−0.13185+2	0.20714+2	0.36965+2		0.24340
$^1S_0$	−0.11106+1	0.60138	−0.12580+1	0.56438	0.98593	0.12768+1	−0.22425+1	0.14022	0.42953+2	
$^3P_0$	0.13967	−0.11469	−0.17595	−0.56536	0.52938	−0.73959	0.12821+1	0.15717+1	0.25103+2	0.32999+2
$^3P_1$	0.15059	−0.48773+1	−0.10619+1	−0.42459+1	−0.10798+1	0.56481+1	−0.29428+1	−0.47056+1	0.58756+1	0.16388+2
$^1D_2$	−0.80323+1	0.10130+1	−0.81856+1	0.62079+1	0.26261+1	0.16422+2	−0.20743+2	−0.11771+2	0.15141+3	0.86249+2
$^3P_2$	0.49471+1	0.12383+1	0.10118+2	−0.10856+2	0.14096+1	−0.98784+1	0.12254+2	0.23105+1	0.10829+1	−0.30574+1
ϵ_2	−0.75172+1	0.21826+1	−0.10368+2	0.10100+2	−0.26557+1	0.20870+2	−0.20081+2	−0.17972+2	0.22408+3	0.21335+3
$^3F_2$	0.34678+1	−0.67365	0.19351+1	−0.32313+1	0.24203+1	−0.90128+1	0.12219+2	0.13306+2	−0.96845+2	−0.10615+3
$^3F_3$	0.57471+1	0.34391	0.99170+1	−0.58028+1	−0.26429+1	−0.79508+1	0.10716+2	−0.29405+1	−0.17933+3	−0.16271+3
$^3F_4$	0.13756−1	−0.28512+1	−0.71318+1	0.13947+1	0.34575+1	−0.84336+1	0.12855+2	0.22717+2	0.26016+3	0.27675+3
$^1G_4$	−0.67778+1	0.88727−1	−0.20046+1	0.44817+1	0.14974+1	0.15766+2	−0.27434+2	−0.19423+2	−0.23567+2	−0.11147+3
ϵ_4	0.35035+1	−0.15726+1	0.12353+2	−0.54953+1	0.51646	−0.51056+1	−0.10269+2	−0.20455+2	−0.35839+3	−0.48036+3

improvements in the (p,p) data measurements over the next few years will not appreciably change the elastic $I=1$ phase-shift solution, but we believe that improvements in the (n,p) data measurements in the near future will have a substantial effect on the elastic $I=0$ amplitudes. The use of fixed $I=1$ amplitudes allows us to extract most of the physical information contained in the present (n,p) elastic scattering data, and improvements in the $I=0$ amplitudes will come mainly from improvements in the (n,p) data, and not from improved handling of the $I=1$ amplitudes.

In Paper VII we described energy-dependent solutions obtained by fitting to a set of 839 (p,p) elastic scattering data. 23 free parameters, representing the phases, gave a χ^2 value of 858, while 30 or more free parameters gave a χ^2 value of 810. Since the 23-parameter solution gave a better extrapolation to higher energies than did the 30-parameter solution, we thought that the local wiggles developed in the latter were not of physical significance, even if they lowered χ^2 somewhat. Hence we adopted the 23-parameter solution as being the most meaningful one. In the present work, we fixed the $I=1$ phases at the values obtained from the 23-parameter search.

To represent the $I=0$ phases, we used the form A energy dependence as described in Paper VII. 912 (n,p) data were used, as described in Tables I and II, extending from 7 to 400 MeV. Search problems using 29, 22, and 19 free parameters gave χ^2 values of 1014, 1032, and 1043, respectively. We judged the 22- and 19-parameter solutions to be the most significant ones. The 22-parameter solution included all $I=0$ phases up through the G waves. The 19-parameter solution excluded the $^3G_3$, $^3G_4$, and $^3G_5$ phases from the search. On a χ^2 basis, it would be difficult to choose between the 19- and 22-parameter solutions. However, when we extended the (n,p) analysis to energies above 400 MeV, as described in Sec. V, the 22-parameter solution gave a much better fit over the entire energy range. Also, from the (p,p) results, G waves certainly deviate appreciably from the one-pion-exchange (OPE) values at energies well below 400 MeV. Thus we adopted the 22-parameter solution as the best representation of the $I=0$ phases. Table XIII gives tabulated values of the $I=0$ phases with uncertainties as determined from the parameter error matrix. These phases are also given graphically in Fig. 1.

The $I=0$ phases of Table XIII should be combined with the $I=1$ phases of Table V in Paper VII to give a complete representation of the nucleon-nucleon elastic scattering matrix. This combined solution represents a fit to 839 (p,p) data plus 912 (n,p) data, or 1751 data in all. The χ^2 value for the combined solution is 1890, and the M value is 1.08. The fact that only 45 free parameters are needed to represent the energy dependence of the 25 phases included in the search is a powerful argument for the plausibility of the energy-dependent forms that were used. The solution gives precision fits to the (p,p) data over the energy range from about 2.5 to 400 MeV. At energies below 2.5 MeV, the (p,p) data require a more accurate treatment of vacuum polarization effects than we have provided. The lowest-energy (n,p) data included are at 7.2 MeV. The form for $^3S_1$ has as the low-energy limit the effective-range expansion, thus giving the correct isoscalar amplitudes at low energies. Since we used the (p,p) effective-range expansion for $^1S_0$ as the low-energy limit, we should not expect to fit (n,p) total cross sections at very low energies. Examination shows that our solution gives a fit to (n,p) total cross sections that is within experimental error for energies of 4 MeV and above. At lower energies, charge-dependent effects in the $^1S_0$ phase lead to some disagreement.

in deg^2) for the 142-MeV solution of Table IV (both $I=0$ and $I=1$ phases included in the search).

$^3P_1$	$^1D_2$	$^3P_2$	ϵ_2	$^3F_2$	$^3F_3$	$^3F_4$	$^1G_4$	ϵ_4	
0.19151−3	0.30134−1	−0.84814−2	0.11379−2	−0.66250−1	0.43216−1	−0.27941−1	−0.11066−1	−0.16972−2	$^1P_1$
−0.11133−1	0.59730−2	−0.46865−2	−0.70305−2	0.38210−1	−0.21199−1	0.19443−1	0.26862−2	−0.14913−2	$^3S_1$
−0.11366−1	−0.10432−1	−0.45986−2	−0.12752−2	0.35007−1	−0.21255−1	0.16115−1	0.23218−2	0.60480−3	ϵ_1
0.16265−1	−0.60683−2	0.78238−2	0.27564−2	−0.21796−1	0.62650−2	−0.12802−1	−0.46526−3	0.17786−2	$^3D_1$
0.19950−1	0.59930−2	0.28300−2	0.69658−2	−0.68990−1	0.36983−1	−0.33139−1	−0.62942−2	0.12607−2	$^3D_2$
−0.94931−2	−0.70884−2	−0.48520−2	−0.14893−2	0.13944−1	−0.94526−2	0.85737−2	0.15166−2	0.91802−3	$^3D_3$
0.71651−2	−0.91420−2	0.28214−2	−0.22458−3	−0.13820−2	−0.67291−2	−0.17197−2	0.21460−2	0.17554−2	$^1F_3$
0.47205−2	0.44866−2	0.12874−2	0.20575−2	−0.18863−1	0.11477−1	−0.89639−2	−0.28626−2	0.40583−3	ϵ_3
0.25817−1	−0.55150−1	−0.23792−2	0.19753−1	−0.71635−1	0.46460−1	−0.29066−1	0.49251−2	0.56154−2	$^1S_0$
0.40728−1	−0.10422−1	0.15430−1	0.38226−2	−0.80083−1	0.28855−1	−0.39971−1	−0.28281−2	0.72030−2	$^3P_0$
0.25228−1	−0.14696−2	0.11715−1	0.99104−3	−0.16559−1	0.23329−2	−0.11610−1	0.30081−3	0.12783−2	$^3P_1$
	0.28214−1	0.85258−3	−0.72147−2	−0.35505−2	0.23079−2	−0.33004−2	−0.67013−2	−0.21095−2	$^1D_2$
0.15626+3		0.11063−1	0.25434−3	−0.31183−2	−0.24369−2	−0.46360−2	0.78658−3	0.20553−3	$^3P_2$
0.19121+2	0.75999+3		0.45186−2	−0.30508−2	0.33286−2	−0.13431−2	0.12253−2	0.54247−3	ϵ_3
−0.91952+2	−0.94360+2	0.27328+3		0.52348−1	−0.25751−1	0.23729−1	0.48697−2	−0.22654−2	$^3F_2$
0.19503+3	0.93660+3	−0.73168+2	0.23762+4		0.24852−1	−0.86258−2	−0.10471−2	−0.96325−3	$^3F_3$
−0.13065+3	−0.24109+3	−0.85541+2	−0.11630+4	0.10999+4		0.13991−1	0.30272−2	−0.87174−3	$^3F_4$
−0.13352+3	−0.58451+3	0.55545+1	−0.15992+4	0.11067+4	0.14251+4		0.40372−2	−0.52206−3	$^1G_4$
0.32686+3	0.73120+3	0.16066+3	0.25257+4	−0.19514+4	−0.21758+4	0.41452+4		0.11421−2	ϵ_4
−0.21372+3	0.37003+3	−0.22028+3	−0.75823+3	0.91053+3	0.79192+3	−0.18934+4	0.21479+4		
−0.56400+3	−0.57382+3	−0.20764+3	−0.41206+4	+0.34456+4	0.38412+4	−0.67025+4	0.41708+4	0.14130+5	

TABLE IX. Second-derivative matrix (below the diagonal, in deg^{-2}) and error matrix (above the diagonal, in deg^2) for the 210-MeV solution of Table IV (both $I=0$ and $I=1$ phases included in the search).

	$^1P_1$	$^3S_1$	ϵ_1	$^3D_1$	$^3D_2$	$^3D_3$	$^1F_3$	ϵ_3	
	0.35100+1	0.12526+1	−0.71439	−0.10581+1	0.84991−1	0.28600	−0.11160+1	0.21960	$^1P_1$
		0.17969+1	−0.12921	−0.15701+1	−0.68883	−0.12663	−0.56781	0.93800−1	$^3S_1$
$^1P_1$	0.29684+1		0.50479	0.12206	−0.30927	−0.12670	0.10079	0.44664−1	ϵ_1
$^3S_1$	−0.15386+1	0.28210+1		0.20706+1	0.92786	0.41675	0.81688	−0.13815	$^3D_1$
ϵ_1	0.24317+1	−0.12736+1	0.69891+1		0.10426+1	0.37249	0.32619	−0.80044−1	$^3D_2$
$^3D_1$	−0.15474+1	0.23326+1	−0.26764+1	0.38480+1		0.66607	0.31699	−0.40633−1	$^3D_3$
$^3D_2$	0.27656	0.92964−1	0.26098+1	−0.15521+1	0.33713+1		0.76181	−0.16124	$^1F_3$
$^3D_3$	−0.30973+1	0.74256	−0.10853+1	0.74799	−0.85357	0.70812+1		0.12787	ϵ_3
$^1F_3$	0.58176+1	−0.25908+1	0.30101+1	−0.39503+1	0.54949	−0.82322+1	0.17539+2		
ϵ_3	0.13001	0.35874	−0.45117+1	0.11156+1	−0.50268	−0.44214+1	0.58502+1	0.20470+2	
$^1S_0$	−0.12697+1	0.63300	−0.15170+1	0.94069	−0.41258	0.10262+1	−0.24585+1	0.59794	
$^3P_0$	−0.22998−1	0.14687	−0.11072+1	0.34850	−0.22234	−0.53000	0.49440	0.16560+1	
$^3P_1$	−0.60064	−0.80853	−0.14629+1	0.24641	−0.17169+1	0.14828+1	−0.16718+1	0.35185	
$^1D_2$	−0.43255+1	0.18524+1	−0.22243+1	0.22272+1	−0.31998	0.56609+1	−0.11147+2	−0.43708+1	
$^3P_2$	0.33462+1	−0.26808+1	0.49589+1	−0.47209+1	0.28874+1	−0.31960+1	0.77060+1	−0.55749	
ϵ_2	−0.34000+1	0.20892+1	−0.41328+1	0.17826+1	−0.25232+1	0.59490+1	−0.66396+1	−0.71691+1	
$^3F_2$	0.24292+1	−0.15460+1	0.14314+1	−0.18076+1	0.15027+1	−0.43774+1	0.65655+1	0.36800+1	
$^3F_3$	0.40251+1	−0.22562+1	0.78630+1	−0.41141+1	0.21734+1	−0.67849	0.57828+1	−0.91464+1	
$^3F_4$	−0.80463	0.10820+1	−0.68644+1	0.19178+1	−0.24124+1	−0.37592+1	0.51077+1	0.13314+2	
$^1G_4$	−0.54468+1	0.21695+1	−0.13429+1	0.37766+1	−0.65533	0.88489+1	−0.19492+2	−0.60293+1	
ϵ_4	0.24625+1	−0.20242+1	0.10604+2	−0.18728+1	0.50760+1	0.91071	−0.60671+1	−0.16185+2	
$^3H_4$	−0.10036+1	0.13646+1	−0.36730+1	0.16916	−0.24108+1	0.78370	0.50340+1	0.38958+1	
$^3H_5$	0.32200+1	−0.10096+1	−0.84830	0.18433	0.62967	−0.71768+1	0.73040+1	0.11171+2	
$^3H_6$	0.15721+1	−0.66486	0.33838+1	−0.30043+1	0.19802+1	−0.77133	0.65418+1	−0.10620+2	

	$^1S_0$	$^3P_0$	$^3P_1$	$^1D_2$	$^3P_2$	ϵ_2	$^3F_2$	
	−0.97065−1	−0.13218	−0.82129−1	−0.86374−1	−0.64801−1	−0.63410−1	0.67464−1	$^1P_1$
	−0.44758−1	−0.51247−1	0.34464−3	−0.77396−2	−0.28233−1	−0.20909−1	0.54048−1	$^3S_1$
	−0.10242−1	0.15042−1	0.14427−1	0.11498−1	0.23308−2	0.96476−2	−0.12405−2	ϵ_1
	0.27166−1	0.20974−1	0.54791−1	0.50475−1	0.60485−1	0.37778−1	−0.43417−1	$^3D_1$
	0.73349−2	−0.15327−1	0.47209−1	0.65275−2	0.99239−3	0.15500−1	−0.10670−1	$^3D_2$
	−0.17043−1	−0.79326−1	−0.37582−2	0.24535−1	−0.16929−1	−0.68993−2	0.63778−1	$^3D_3$
	0.34866−1	0.42539−2	0.72136−1	0.72888−1	0.27713−1	0.36156−1	−0.17495−2	$^1F_3$
	−0.23658−2	0.31867−1	−0.47802−2	−0.14638−1	0.61287−2	0.36842−2	−0.31638−1	ϵ_3
	0.27442	0.48999−1	−0.24075−1	−0.72437−1	−0.53787−3	−0.76056−3	−0.14581−1	$^1S_0$
		0.28814	0.25323−1	−0.12782−1	0.28555−1	−0.17607−2	−0.10666	$^3P_0$
$^1S_0$	0.18174+2		0.95056−1	0.27219−1	0.19737−1	0.24328−1	−0.24608−1	$^3P_1$
$^3P_0$	−0.33937	0.13792+2		0.73151−1	0.20343−1	0.15606−1	−0.31383−2	$^1D_2$
$^3P_1$	0.61813	−0.50492+1	0.30935+2		0.47498−1	0.11071−1	−0.31997−1	$^3P_2$
$^1D_2$	0.31814+2	−0.14638+1	−0.18588+2	0.13567+3		0.23157−1	−0.10978−1	ϵ_2
$^3P_2$	−0.36373+1	−0.43873	0.13410+2	−0.28960+2	0.80448+2		0.86915−1	$^3F_2$
ϵ_2	0.15428+2	0.18973+2	−0.26437+2	0.35330+2	−0.77141+1	0.15579+3		
$^3F_2$	−0.11415+2	0.67992+1	−0.15101+1	−0.86516+1	0.52992	−0.28821+2	0.92332+2	
F_3	−0.31451+2	−0.10307+2	0.18281+2	−0.53940+2	0.29904+2	−0.71596+2	0.59959+2	

TABLE IX. (*continued*).

	$^1S_0$	$^3P_0$	$^3P_1$	$^1D_2$	$^3P_2$	ϵ_2	$^3F_2$	
$^3F_4$	0.23791+2	0.22490+2	0.28791+2	−0.26069+2	0.98736+2	0.99158+2	−0.11027+3	
$^1G_4$	0.36404+1	0.16560	−0.58630+2	0.14270+3	−0.68516+2	0.55554+2	−0.40007+1	
ϵ_4	0.63800+1	−0.44970+2	−0.17774+2	0.13322+3	−0.26275+2	−0.91047+2	0.10211+3	
$^3H_4$	0.50183+1	−0.15984+1	0.86609+1	−0.28113+2	−0.73876+1	0.43211+2	−0.14438+2	
$^3H_5$	−0.21606+2	0.97798+1	0.57390+1	−0.93804+2	0.10143+2	−0.18571+2	0.33418+2	
$^3H_6$	0.10297+2	0.18000+2	0.10726+2	0.53485+2	0.74032+2	0.82646+1	0.59709+2	
	$^3F_3$	$^3F_4$	$^1G_4$	ϵ_4	$^3H_4$	$^3H_5$	$^3H_6$	
	−0.74709−1	0.21360−1	0.15845−1	−0.10457−1	0.12251	−0.10493	0.72040−1	$^1P_1$
	−0.37655−1	0.28659−1	0.16342−2	0.57232−2	0.10105−2	−0.34347−2	0.18146−2	$^3S_1$
	−0.36076−2	−0.13039−2	−0.44851−2	0.20114−2	−0.98733−2	0.12369−1	−0.49482−2	ϵ_1
	0.30666−1	−0.37065−1	−0.28063−2	−0.14185−1	−0.34890−1	0.34226−1	−0.18385−1	$^3D_1$
	0.94313−2	−0.99076−2	0.71049−2	−0.86774−2	−0.47138−2	0.17402−2	−0.96408−3	$^3D_2$
	−0.18392−1	0.35592−1	−0.13308−2	−0.30805−3	−0.41198−1	0.25500−1	−0.24318−1	$^3D_3$
	0.25989−1	0.20217−2	−0.51713−2	−0.12445−2	−0.91267−1	0.73457−1	−0.51071−1	$^1F_3$
	0.51314−2	−0.18379−1	−0.11378−2	0.95539−3	0.26220−1	−0.17279−1	0.16656−1	ϵ_3
	0.58139−1	−0.60180−2	0.22923−1	−0.29632−2	−0.99434−2	−0.76508−2	−0.43153−2	$^1S_0$
	0.34397−1	−0.36187−1	−0.65750−2	0.22004−1	0.22611−1	−0.51815−2	0.45565−2	$^3P_0$
	−0.46569−2	−0.21041−1	0.15094−2	−0.19518−2	−0.15523−1	0.23858−1	−0.38059−2	$^3P_1$
	0.21663−3	−0.69699−2	−0.17259−1	−0.58449−2	−0.26125−1	0.29087−1	−0.16659−1	$^1D_2$
	0.60639−3	−0.27865−1	−0.28753−2	−0.44690−2	−0.27431−2	0.14191−1	0.25516−3	$^3P_2$
	0.87274−2	−0.10043−1	−0.40160−2	−0.15723−2	−0.13411−1	0.12076−1	−0.60538−2	ϵ_2
	−0.16328−1	0.39853−1	0.38348−2	−0.47116−2	−0.13611−1	−0.73236−2	−0.10813−1	$^3F_2$
	0.38468−1	−0.25413−2	−0.30912−3	−0.78267−3	−0.93608−2	−0.11143−2	−0.87565−2	$^3F_3$
		0.30670−1	0.15049−2	0.40081−2	−0.70718−2	−0.62468−2	−0.80194−2	$^3F_4$
$^3F_3$	0.14919+3		0.99991−2	−0.14389−2	0.41904−2	−0.43492−2	0.42760−2	$^1G_4$
$^3F_4$	−0.63402+2	0.46334+3		0.74497−2	0.25332−2	−0.11439−2	−0.42709−3	ϵ_4
$^1G_4$	−0.57619+2	−0.16007+3	0.42102+3		0.37092−1	−0.22964−1	0.19794−1	$^3H_4$
ϵ_4	0.80724+2	−0.35318+3	0.21236+3	0.67724+3		0.29745−1	−0.10247−1	$^3H_5$
$^3H_4$	−0.11592+2	0.62742+2	−0.31492+2	−0.13578+3	0.22746+3		0.14972−1	$^3H_6$
$^3H_5$	0.63240+2	0.46502+2	−0.95242+2	−0.12195+3	0.99898+2	0.19685+3		
$^3H_6$	0.90600+2	0.13288+3	−0.10686+3	0.98087+2	−0.20276+3	−0.21948+2	0.60519+3	

TABLE X. Second-derivative matrix (below the diagonal, in deg^{-2}) and error matrix (above the diagonal, in deg^2) for the 330-Mev solution of Table IV (both $I=0$ and $I=1$ phases included in the search).

	$^1P_1$	$^3S_1$	ϵ_1	$^3D_1$	$^3D_2$	$^3D_3$	$^1F_3$	
	0.38424+1	−0.25519	−0.19438	−0.31874	0.32413	−0.49308	−0.96979	$^1P_1$
		0.46147+1	−0.22091+1	−0.27913+1	−0.28766+1	−0.68322	−0.27210−1	$^3S_1$
$^1P_1$	0.10669+1		0.69078+1	0.28201+1	−0.71966	0.18414	0.71845	ϵ_1
$^3S_1$	0.12628	0.21290+1		0.33163+1	0.15583+1	0.91311	0.34142	$^3D_1$
ϵ_1	0.61271	0.34065	0.36991+1		0.47506+1	0.10680+1	−0.12124	$^3D_2$
$^3D_1$	0.29201	0.13672+1	0.99343	0.29079+1		0.14686+1	0.31992	$^3D_3$
$^3D_2$	−0.13738	0.11800+1	−0.25296+1	−0.13895+1	0.54085+1		0.56453	$^1F_3$
$^3D_3$	−0.40676	−0.12621+1	0.30699+1	0.14497+1	−0.64274+1	0.99185+1		
$^1F_3$	0.12868−1	−0.18644	−0.11914+2	−0.59398+1	0.14241+2	−0.18515+2	0.55717+2	
ϵ_3	0.28529	−0.93958	−0.30397+1	−0.23698+1	0.62524+1	−0.68081+1	0.18607+2	
$^3G_3$	0.85431	−0.42827−2	0.50710+1	0.28274+1	−0.57533+1	0.73087+1	−0.20738+2	
$^3G_4$	−0.19832+1	−0.73252	−0.47032+1	−0.14614+1	0.13442+1	−0.37882	0.10632+2	
$^3G_5$	0.16533+1	0.33126	0.57743+1	0.18868+1	−0.32820+1	0.26378+1	−0.17218+2	
$^1S_0$	−0.23261	0.61899−1	0.10481	0.41125	−0.71723	0.11139+1	−0.27943+1	
$^3P_0$	−0.10838	−0.98999−1	−0.10139+1	−0.24430	0.87648	−0.10581+1	0.35188+1	
$^3P_1$	0.97093−1	−0.15591+1	0.14741+1	−0.10118−1	−0.36269+1	0.42336+1	−0.84309+1	
$^1D_2$	−0.25047	0.22874	0.55834+1	0.29236+1	−0.66971+1	0.90598+1	−0.26738+2	
$^3P_2$	−0.34248−2	−0.84734	−0.14040+1	−0.30510+1	0.28344+1	−0.37552+1	0.94938+1	
ϵ_2	−0.10655+1	0.27022	−0.10409+1	0.33623	−0.18769+1	0.26917+1	−0.19026+1	
$^3F_2$	−0.26862	−0.10855+1	−0.37568+1	−0.25046+1	0.41922+1	−0.54249+1	0.15909+2	
$^3F_3$	0.87796	−0.35137	0.48829+1	0.16918+1	−0.53254+1	0.60083+1	−0.18382+2	
$^3F_4$	−0.65962	−0.99405−1	−0.50176+1	−0.24620+1	0.60685+1	−0.76291+1	0.22034+2	
$^1G_4$	0.13147+1	−0.35426	0.15375+2	0.65422+1	−0.16912+2	0.20957+2	−0.65013+2	
ϵ_4	0.79753	−0.51656	0.57908+1	0.16068+1	−0.51419+1	0.56617+1	−0.21342+2	
$^3H_4$	−0.16325+1	0.54940	−0.46870+1	−0.16350+1	0.37061+1	−0.49901+1	0.16165+2	
$^3H_5$	0.24535+1	0.40674	0.24386+1	−0.62137−1	0.24069+1	−0.47262+1	0.20855+1	
$^3H_6$	−0.23524+1	0.13329	−0.41596+1	−0.27211	0.21150−1	0.14943+1	0.60745+1	

TABLE X. (*continued*).

	ϵ_3	$^3G_3$	$^3G_4$	$^3G_5$	$^1S_0$	$^3P_0$	
	0.51876	−0.30972	0.12077+1	−0.56837−1	−0.51259	0.86190−1	$^1P_1$
	0.53201	0.14182+1	−0.64086−1	0.26970	−0.47029	0.14862−1	$^3S_1$
	0.93979−1	−0.21713+1	0.13339+1	−0.30109	0.13077+1	0.20716	ϵ_1
	−0.28509	−0.18487+1	−0.19625	−0.22303	0.24789	0.91729−1	$^3D_1$
	−0.57257	0.18056−1	−0.24212	0.75329−1	−0.24218	0.16046	$^3D_2$
	−0.37674	−0.10375+1	−0.96401	0.33645−1	0.14454	−0.12149	$^3D_3$
	−0.19449	−0.15369−1	−0.14685	0.99258−1	0.37891	−0.45738−3	$^1F_3$
	0.35436	0.12135	0.36400	−0.63848−2	−0.15917	0.14661	ϵ_3
		0.29052+1	0.74392	0.30418	−0.30280	−0.67766−1	$^3G_3$
ϵ_3	0.23776+2		0.21420+1	0.35120	0.93141−1	0.14790−1	$^3G_4$
$^3G_3$	−0.56196+1	0.95506+1		0.44837	−0.53742−2	−0.22656−1	$^3G_5$
$^3G_4$	−0.27674+1	−0.59237+1	0.10446+2		0.19483+1	0.29346	$^1S_0$
$^3G_5$	−0.30640	0.76842+1	−0.10598+2	0.14325+2		0.24000+1	$^3P_0$
$^1S_0$	−0.13420+1	0.67562	0.53128	−0.13542	0.30851+1		
$^3P_0$	0.14121+1	−0.14349+1	0.10495+1	−0.14452+1	0.72463	0.17328+1	
$^3P_1$	−0.40627+1	0.31505+1	−0.21526	0.14959+1	−0.10436+1	−0.13096+1	
$^1D_2$	−0.91848+1	0.99954+1	−0.45119+1	0.76497+1	0.22501+1	−0.51747	
$^3P_2$	0.37676+1	−0.40170+1	0.58328	−0.14843+1	−0.11793+1	−0.63189	
ϵ_2	−0.10430+2	−0.43549	0.59731+1	−0.51387+1	0.66198+1	0.21246+1	
$^3F_2$	0.67668+1	−0.62976+1	0.32344+1	−0.47581+1	−0.59381+1	0.82063	
$^3F_3$	−0.58273+1	0.80402+1	−0.59953+1	0.78774+1	−0.79477+1	−0.52586+1	
$^3F_4$	0.87383+1	−0.93277+1	0.50680+1	−0.82994+1	0.92564+1	0.49241+1	
$^1G_4$	−0.14419+2	0.25894+2	−0.17954+2	0.25103+2	0.80940+1	−0.26139+1	
ϵ_4	−0.10933+2	0.81408+1	−0.71431+1	0.10187+2	−0.45180+1	−0.19047+1	
$^3H_4$	−0.30625+1	−0.79941+1	0.91943+1	−0.10505+2	0.13613+1	0.10117	
$^3H_5$	0.14696+2	0.13843+1	−0.11440+2	0.95447+1	−0.62131+1	−0.21585+1	
$^3H_6$	−0.11360+2	−0.42428+1	0.12407+2	−0.12271+2	0.66924+1	0.54505+1	

	$^2P_1$	$^1D_2$	$^3P_2$	ϵ_2	$^3F_2$	$^3F_3$	
	−0.51039	−0.51135−1	0.16922−1	−0.68990−1	−0.12160	0.12221	$^1P_1$
	0.54482	−0.21590	0.12591	−0.15883	0.22028	−0.26128	$^3S_1$
	−0.71561	−0.66599−2	0.96368−1	−0.33063−1	0.13211	0.19659	ϵ_1
	0.16701	0.11342	0.29295	0.67124−1	0.21858−1	0.78195−2	$^3D_1$
	0.80358	0.17172	−0.49062−1	0.26374	−0.25617	0.64925−1	$^3D_2$
	0.11795	0.68580−1	0.12271−1	0.77600−2	0.89085−1	−0.28802−1	$^3D_3$
	0.14027	0.66663−1	0.25914−2	−0.53572−2	0.28115−1	0.47529−2	$^1F_3$
	−0.10704−1	−0.75887−1	0.59610−1	−0.26795−1	−0.46840−1	0.31206−1	ϵ_3
	0.34822	−0.78789−1	−0.44252−1	0.22429−1	−0.15952−1	−0.14523	$^3G_3$
	−0.32894	−0.29086−1	−0.36402−1	0.30025−1	−0.87681−1	0.32033−1	$^3G_4$
	0.74695−1	0.79208−2	−0.29546−1	0.13056−1	0.92503−2	−0.10477−1	$^3G_5$
	−0.45585	−0.95638−1	−0.12317	−0.10623	−0.12940−1	0.41471	$^1S_0$
	0.97463−1	−0.11029	0.29757	−0.12854	−0.47747	0.52236	$^3P_0$
	0.13453+1	0.54505−1	0.17482	0.12604	−0.16461−1	−0.26925	$^3P_1$
		0.22887	−0.11973−1	0.60228−1	−0.34317−1	−0.48210−1	$^1D_2$
$^3P_1$	0.53750+1		0.30114	−0.50868−1	−0.17251−1	−0.37441−1	$^3P_2$
$^1D_2$	0.34991+1	0.34015+2		0.17000	0.18756−2	−0.35114−1	ϵ_2
$^3P_2$	−0.11175+1	−0.67365+1	0.11215+2		0.30580	−0.14332	$^3F_2$
ϵ_2	−0.40058+1	0.17181+1	−0.19175+1	0.32148+2		0.35061	$^3F_3$
$^3F_2$	0.18659+1	0.58846+1	0.35575+1	−0.15658+2	0.40059+2		
$^3F_3$	0.98179+1	0.14138+2	0.18336+1	−0.22135+2	0.23474+2	0.48970+2	
$^3F_4$	−0.10581+2	−0.35345+2	0.75187+1	0.25979+2	−0.52341+2	−0.61365+2	
$^1G_4$	0.37171+1	0.26994+2	−0.12616+2	0.14907+2	−0.40457+2	−0.80182	
ϵ_4	0.74826+1	0.50692+2	−0.49217+1	−0.14633+2	0.45444+2	0.48436+2	
$^3H_4$	−0.48663+1	−0.39213+2	0.50437+1	0.15630+2	−0.24890+2	−0.25316+2	
$^3H_5$	0.74516	−0.19904+2	0.85085+1	−0.24617+2	0.10866	0.15653+2	
$^3H_6$	−0.19970+1	0.39090+2	0.21715+1	0.21316+2	0.25646+2	−0.13528+1	

	$^3F_4$	$^1G_4$	ϵ_4	$^3H_4$	$^3H_5$	$^3H_6$	
	0.40721−1	−0.24549−1	0.80885−1	0.12544	−0.17369	0.22947−1	$^1P_1$
	0.12498	0.20376−1	0.17719	0.17935	−0.22735	0.34445−1	$^3S_1$
	−0.41441−1	−0.75913−1	−0.13271	−0.18864	0.90163−1	−0.10215	ϵ_1
	−0.85187−1	0.51426−1	−0.13313	−0.11054	0.29228−1	−0.42129−1	$^3D_1$
	−0.12762	0.12637	−0.10288	−0.92433−1	0.19363	0.33145−1	$^3D_2$
	−0.11003−1	0.18842−1	−0.65000−1	−0.22191−1	0.23470−1	−0.37680−2	$^3D_3$
	−0.22255−1	0.25935−1	−0.46562−1	−0.54161−1	0.69331−1	−0.15460−1	$^1F_3$
	0.18159−1	−0.15216−1	0.63685−1	0.76929−1	−0.11199	0.95954−2	ϵ_3
	0.32536−1	0.15490−1	0.10791	0.42156−1	0.54240−1	0.32063−1	$^3G_3$
	−0.48895−2	−0.21254−1	0.46619−1	−0.64676−1	0.14085	−0.12179−1	$^3G_4$
	0.10586−1	−0.28058−2	0.57201−2	0.53463−2	0.16026−1	0.50357−2	$^3G_5$
	−0.11759−1	−0.81403−1	−0.56505−1	−0.92472−1	0.40408−1	−0.72009−1	$^1S_0$
	−0.88167−1	−0.10469−2	0.72331−2	0.66439−1	−0.27730	−0.43655−1	$^3P_0$
	−0.52007−1	0.10083	0.17969−1	0.34528−1	0.30455−1	0.39724−1	$^3P_1$
	−0.17197−1	−0.32678−1	−0.47606−1	−0.24572−1	0.94907−1	−0.14147−1	$^1D_2$

TABLE X. (*continued*).

	$^3F_4$	$^1G_4$	ϵ_4	$^3H_4$	$^3H_5$	$^3H_6$	
	−0.20220−1	0.24987−1	0.33006−2	0.24004−1	−0.10854	−0.13813−1	$^3P_2$
	−0.15721−1	−0.15699−1	−0.20275−1	−0.49943−1	0.10911	−0.59306−2	ϵ_2
	0.68064−1	0.17749−1	−0.19380−1	−0.20853−1	−0.55092−2	−0.75355−2	$^3F_2$
	0.87304−2	−0.15758−1	−0.18849−1	0.16804−2	−0.10492	−0.24656−1	$^3F_3$
	0.47423−1	−0.35695−2	0.10670−1	0.70389−2	−0.32809−1	−0.46106−2	$^3F_4$
		0.58197−1	0.77014−4	0.18466−2	−0.19173−1	0.12982−1	$^1G_4$
$^3F_4$	0.15086+3		0.49937−1	0.34860−1	−0.17162−1	0.11041−1	ϵ_4
$^1G_4$	0.12976+2	0.13211+3		0.74122−1	−0.69467−1	0.18233−1	$^3H_4$
ϵ_4	−0.11149+3	−0.39734+1	0.15684+3		0.22588	0.83762−2	$^3H_5$
$^3H_4$	0.65308+2	0.91676+1	−0.97633+2	0.11922+3		0.20685−1	$^3H_6$
$^3H_5$	0.12108+2	0.85161+1	−0.28457+2	0.31897+2	0.59895+2		
$^3H_6$	−0.26590+2	−0.54707+2	0.69798+2	−0.99560+2	−0.76397+2	0.24706+3	

TABLE XI. Second-derivative matrix (below the diagonal, in deg^{-2}) and error matrix (above the diagonal, in deg^2) for the 11-parameter 425-MeV solution of Table XV. The matrices are given as the direct product of an isovector matrix with an isoscalar matrix. In calculating with these matrices, the $^1D_2$ phase shift should be assigned a (fixed) imaginary value of 23.46°, as defined in Eq. (5) of Paper VIII and shown in solution 2 of Table V in Paper VIII.

Isovector ($I=1$) matrices

	$^1S_0$	$^3P_0$	$^3P_1$	$^3P_2$	ϵ_2	$^1D_2$	$^3F_2$	$^3F_3$	
	0.42151+1	0.13670+1	0.18588+1	0.12903+1	−0.50260−1	0.21919+1	0.10500+1	0.89320	$^1S_0$
		0.71942+1	0.22232+1	0.23599+1	0.16786+1	0.54060	0.24492+1	0.83901	$^3P_0$
$^1S_0$	0.13498+1		0.19732+1	0.10433+1	0.29784	0.75923	0.86040	0.48474	$^3P_1$
$^3P_0$	−0.17190	0.17321+1		0.17024+1	0.31077	0.10653+1	0.12766+1	0.59150	$^3P_2$
$^3P_1$	−0.51473	−0.39315	0.17495+1		0.79597	−0.56825−1	0.52756	0.10591	ϵ_2
$^3P_2$	0.12513+1	−0.48803	0.26980	0.58471+1		0.18414+1	0.82885	0.62907	$^1D_2$
ϵ^2	0.14094−1	−0.31340+1	−0.62775	−0.49075	0.13991+2		0.14801+1	0.46314	$^3F_2$
$^1D_2$	−0.11399+1	0.68581	0.46751	−0.15586+1	0.30175	0.42222+1		0.39427	$^3F_3$
$^3F_2$	0.15396−1	−0.33270	0.62341	−0.12735+1	−0.45168+1	−0.30721	0.68924+1		
$^3F_3$	−0.19116+1	−0.30829+1	−0.15304+1	−0.67359+1	0.13745+2	0.25921	−0.15942+1	0.34309+2	
$^3F_4$	−0.79996	−0.58400−1	−0.96688	−0.45019+1	0.31604	−0.11176+1	−0.20355+1	0.57984	
ϵ_4	0.54436	−0.18682+1	0.86248	0.10357+1	0.37839	0.12655+1	0.39927+1	0.37297	
$^1G_4$	−0.86697	0.47600	−0.99503	−0.67600	0.14370−1	−0.29730+1	−0.12514+1	0.49272	
$^3H_4$	0.62258	−0.12571+1	0.30582	0.19323+1	0.66584+1	−0.11791+1	−0.58447+1	0.30367+1	
$^3H_5$	0.15668+1	0.26500+1	0.22451+1	0.61566+1	−0.16714+2	−0.22253+1	0.42355+1	−0.27943+2	
$^3H_6$	−0.32766	0.17386+1	−0.74535	0.19450+1	0.48833	0.10613+1	−0.17994+1	−0.83815	

	$^3F_4$	ϵ_4	$^1G_4$	$^3H_4$	$^3H_5$	$^3H_6$	
	0.84255	−0.11763	0.79579	0.32891	0.23934	0.22402	$^1S_0$
	0.12626+1	0.60050	0.38851	0.67194	0.25256	0.15962	$^3P_0$
	0.57689	0.52308−1	0.37273	0.20858	0.70329−2	0.83258−1	$^3P_1$
	0.76946	0.94933−1	0.38560	0.37747	0.61308−1	0.12527	$^3P_2$
	0.17697	0.10007	0.43998−1	0.13046−1	0.22544	−0.94627−2	ϵ_2
	0.62396	0.94430−1	0.56905	0.30060	0.25504	0.18646	$^1D_2$
	0.72298	0.14263	0.32176	0.48026	0.12347	0.19375	$^3F_2$
	0.34634	0.46834−1	0.22872	0.16672	0.18403	0.98022−1	$^3F_3$
	0.51402	0.13227	0.22920	0.30691	0.10817	0.15082	$^3F_4$
		0.22926	−0.57719−2	0.14948	0.33739−1	0.65625−1	ϵ_4
$^3F_4$	0.19994+2		0.26078	0.10083	0.97123−1	0.61114−1	$^1G_4$
ϵ_4	−0.50318+1	0.13525+2		0.34550	0.30480−1	0.15539	$^3H_4$
$^1G_4$	0.90924	−0.24085+1	0.15197+2		0.27878	0.57000−1	$^3H_5$
$^3H_4$	−0.30366+1	−0.52509+1	0.90857	0.19260+2		0.12173	$^3H_6$
$^3H_5$	−0.28797+1	−0.42239	−0.22189+1	−0.21202+1	0.33646+2		
$^3H_6$	−0.59397+1	−0.17190+1	0.91896	−0.99699+1	−0.44993+1	0.29656+2	

Isoscalar ($I=0$) matrices

	$^1P_1$	$^3S_1$	ϵ_1	$^3D_1$	$^3D_2$	$^3D_3$	
	0.13265+2	0.66228+1	−0.52488+1	−0.79513+1	−0.55126+1	−0.55769	$^1P_1$
		0.84299+1	−0.24378+1	−0.63897+1	−0.72706+1	−0.16899+1	$^3S_1$
$^1P_1$	0.84656		0.67961+1	0.53107+1	0.29174+1	0.83593	ϵ_1
$^3S_1$	0.28855	0.13446+1		0.84222+1	0.61665+1	0.16137+1	$^3D_1$
ϵ_1	0.11926+1	0.49243	0.47832+1		0.14012+2	0.52649+1	$^3D_2$
$^3D_1$	0.10023	0.53684	−0.78039	0.16910+1		0.28655+1	$^3D_3$
$^3D_2$	0.61062−1	0.47750	−0.10046+1	−0.53637−1	0.17184+1		
$^3D_3$	−0.45808	−0.67353	0.39784	−0.24508	−0.24794+1	0.53367+1	
$^1F_3$	0.16188+1	0.90898	0.13326+1	−0.13136+1	0.91289	0.77081−1	
ϵ_3	−0.69991	−0.11867	−0.30631+1	0.15778	0.14888+1	−0.11650+1	
$^3G_3$	0.64469	0.23065	0.32249+1	0.52270	−0.15508+1	0.17008+1	
$^3G_4$	−0.89952	−0.83598	−0.28083+1	0.16573	0.11273	0.78980	
$^3G_5$	0.42432	0.22736	0.20252+1	0.25983	0.41520	−0.32011+1	

TABLE XI. (*continued*).

	$^1F_3$	ϵ_3	$^3G_3$	$^3G_4$	$^3G_5$	
	−0.10392+1	0.13021+1	0.24584+1	0.41999+1	0.18484+1	$^1P_1$
	−0.35198	0.16316+1	0.15492+1	0.54357+1	0.18409+1	$^3S_1$
	0.72390	0.86080	−0.21776+1	0.27550+1	0.62887−1	ϵ_1
	0.78861	−0.73149	−0.24850+1	−0.23121+1	−0.11940+1	$^3D_1$
	0.19005−1	−0.16564+1	−0.84548	−0.43483+1	−0.78510	$^3D_2$
	−0.25836−1	−0.35620	−0.19087	−0.61398	0.36633	$^3D_3$
	0.30441	0.46654−1	−0.31191	0.30358	0.94096−1	$^1F_3$
		0.97852	0.80203−1	0.25604+1	0.64185	ϵ_3
$^1F_3$	0.17316+2		0.14568+1	0.28935	0.38725	$^3G_3$
ϵ_3	0.96802	0.11023+2		0.90930+1	0.25919+1	$^3G_4$
$^3G_3$	0.15237+1	−0.24946+1	0.58683+1		0.12801+1	$^3G_5$
$^3G_4$	−0.14195+1	−0.10814+1	−0.13821+1	0.34909+1		
$^3G_5$	−0.37424+1	0.71548−1	−0.20932	−0.33666+1	0.90550+1	

TABLE XII. Single-energy phase shifts that correspond to the second-derivative (below the diagonal, in deg^{-2}) and error matrices (above the diagonal, in deg^2) shown in Tables V–XI. The phases are listed here in the order that they appear in the matrix tabulations. The equations for using these matrices are given in the Appendix.

Energy (MeV)	25	50	95	142	210	330	425[a]
Matrix table	V	VI	VII	VIII	IX	X	XI
$^1P_1$	−4.15	−0.74	−12.93	17.40	−21.27	−41.14	−39.44
$^3S_1$	85.42	63.18	45.43	30.00	14.16	8.81	8.13
ϵ_1	−0.50	1.62	− 0.12	3.45	6.20	7.24	− 4.85
$^3D_1$	−3.32	−6.02	−11.49	−15.06	−18.10	−30.45	−41.41
$^3D_2$		10.19	14.37	22.74	28.07	17.27	8.65
$^3D_3$		1.21	1.90	2.05	4.25	2.98	− 1.31
$^1F_3$				− 2.62	− 4.30	− 3.76	− 6.01
ϵ_3				4.60	6.49	9.87	8.98
$^3G_3$						− 3.72	1.18
$^3G_4$						1.41	0.39
$^3G_5$						− 0.78	− 1.45
$^1S_0$	48.60	39.52	26.22	16.65	5.53	−10.94	−19.35
$^3P_0$	8.46	11.08	11.21	5.87	− 1.13	−12.24	−18.19
$^3P_1$	−5.06	−8.06	−12.88	−17.07	−22.16	−27.85	−34.63
$^1D_2$	0.76	1.75	3.59	4.99	7.04	9.03	10.91
$^3P_2$	2.47	5.74	9.96	13.71	15.65	16.16	17.18
ϵ_2		−1.73	− 2.55	− 2.85	− 2.85	− 2.63	− 1.43
$^3F_2$		−0.07	0.29	0.72	1.22	0.22	0.87
$^3F_3$		−0.46	− 0.59	− 2.05	− 2.66	− 3.62	− 3.71
$^3F_4$		0.11	0.51	0.93	2.02	2.75	3.31
$^1G_4$				0.79	1.10	1.30	1.42
ϵ_4				− 0.77	− 1.01	− 0.89	− 1.86
$^3H_4$					0.15	1.32	0.08
$^3H_5$					− 0.98	− 1.91	− 2.07
$^3H_6$					0.10	0.74	0.35
($^1D_2$ Im)							(23.46)

[a] The $^1D_2$ and $^1G_4$ phases are not as ordered here for the 425 MeV matrices.

The behavior of the ϵ_1 and $^1P_1$ phases for the Livermore solution at low energies indicates that the experimental (n,p) data near the threshold are not complete. These phases, which might be expected to approximate the OPE-contribution values at low energies, do not do so. We shall discuss this point in detail in Sec. VI. The qualitative correctness of the $I=0$ amplitudes at intermediate energies is indicated by the fact that the behavior of the R_T variable at 200 MeV was correctly predicted prior to the measurements of Thorndike and his coworkers at Rochester.[8]

[8] N. W. Reay *et al.*, reference Rochester (1966) of Table II.

V. PHASE-SHIFT ANALYSIS ABOVE 400 MeV

From the results discussed in Papers VII and VIII, and thus far in the present paper, we know that we are immediately in great difficulties at energies much above 400 MeV. Paper VII gives a phase-shift solution for the $I=1$ phases that is unique and well-defined over the whole elastic energy region. Using these phases and assuming charge independence, we see from the present paper that it is nevertheless still a difficult problem to define the $I=0$ phases reliably in this region. At energies above 425 MeV, however, Paper VIII shows that it is impossible at the present time to determine the $I=1$

TABLE XIII. Phase-shift values from the 22-parameter 0–400-MeV solution. Only the isotopic spin $I=0$ phases are shown here. The $I=1$ phases are those of Table V in Paper VII. The errors are calculated from the parameter error matrix. This solution is discussed in the text. The combined phases give a χ^2 total of 1890 for a fit to 839 (p,p) data and 912 (n,p) data; thus the M value is 1.08 for the combined solution.

Lab energy (MeV)	$^1P_1$	$^1F_3$	$^3S_1$	ϵ_1	$^3D_1$	$^3D_2$
5	− 0.57±0.08	−0.01±0.00	118.52±0.07	−0.46±0.08	− 0.16±0.00	0.27±0.00
10	− 0.79±0.18	−0.08±0.00	103.17±0.16	−1.87±0.17	− 0.64±0.02	0.99±0.01
15	− 0.77±0.27	−0.19±0.00	93.81±0.24	−1.61±0.27	− 1.29±0.04	1.97±0.02
20	− 0.71±0.35	−0.32±0.01	87.01±0.30	−2.03±0.34	− 2.05±0.06	3.07±0.03
25	− 0.70±0.41	−0.47±0.01	81.59±0.34	−2.34±0.40	− 2.84±0.08	4.21±0.04
30	− 0.60±0.45	−0.63±0.02	77.06±0.37	−2.53±0.45	− 3.65±0.11	5.37±0.06
40	− 1.26±0.51	−0.93±0.03	69.61±0.39	−2.63±0.51	− 5.22±0.15	7.64±0.10
50	− 2.37±0.53	−1.21±0.06	63.52±0.38	−2.43±0.53	− 6.70±0.17	9.78±0.13
60	− 3.72±0.53	−1.46±0.08	58.29±0.35	−2.02±0.53	− 8.04±0.19	11.75±0.17
70	− 5.30±0.54	−1.69±0.11	53.67±0.32	−1.47±0.51	− 9.26±0.19	13.56±0.21
80	− 7.04±0.55	−1.90±0.13	49.50±0.31	−0.89±0.50	−10.36±0.19	15.14±0.24
90	− 8.83±0.58	−2.09±0.16	45.71±0.30	−0.15±0.48	−11.35±0.19	16.65±0.27
100	−10.70±0.62	−2.27±0.19	42.21±0.31	0.56±0.46	−12.26±0.19	17.96±0.30
120	−14.32±0.72	−2.59±0.23	35.95±0.35	1.95±0.44	−13.86±0.23	20.14±0.36
140	−17.70±0.83	−2.89±0.27	30.48±0.41	3.23±0.44	−15.26±0.30	21.03±0.42
160	−20.74±0.95	−3.18±0.31	25.65±0.47	4.37±0.46	−16.54±0.38	23.04±0.48
180	−23.39±1.07	−3.46±0.33	21.33±0.56	5.35±0.50	−17.74±0.46	23.99±0.54
200	−25.65±1.19	−3.74±0.35	17.47±0.67	6.15±0.57	−18.91±0.54	24.53±0.62
220	−27.53±1.31	−4.04±0.36	13.98±0.82	6.79±0.67	−20.07±0.61	24.92±0.70
240	−29.65±1.45	−4.33±0.37	10.81±1.01	7.27±0.80	−21.25±0.69	25.04±0.78
260	−30.23±1.59	−4.64±0.38	7.94±1.23	7.61±0.95	−22.44±0.76	24.98±0.88
280	−31.10±1.75	−4.85±0.40	5.33±1.48	7.81±1.13	−23.67±0.84	24.76±0.98
300	−31.69±1.93	−5.28±0.43	2.94±1.75	7.90±1.32	−24.94±0.94	24.41±1.08
320	−32.03±2.12	−5.61±0.46	0.75±2.05	7.88±1.53	−26.25±1.04	23.95±1.19
340	−32.14±2.32	−5.94±0.50	−1.26±2.36	7.76±1.76	−27.60±1.17	23.39±1.30
360	−32.04±2.54	−6.29±0.56	−3.11±2.68	7.57±1.99	−28.94±1.31	22.75±1.41
380	−31.76±2.76	−6.69±0.62	−4.81±3.02	7.29±2.24	−30.42±1.47	22.05±1.53
400	−31.31±3.00	−6.99±0.69	−6.37±3.36	6.94±2.49	−31.89±1.65	21.28±1.65

Lab energy (MeV)	$^3D_3$	ϵ_3	$^3G_3$	$^3G_4$	$^3G_5$
5	0.01±0.00	0.02±0.00	−0.00±0.00	0.00±0.00	−0.00±0.00
10	0.03±0.00	0.10±0.00	−0.00±0.00	0.02±0.00	−0.00±0.00
15	0.07±0.01	0.24±0.00	−0.02±0.00	0.05±0.00	−0.00±0.00
20	0.12±0.02	0.43±0.00	−0.04±0.00	0.12±0.00	−0.01±0.00
25	0.18±0.03	0.64±0.00	−0.06±0.00	0.20±0.00	−0.01±0.00
30	0.25±0.04	0.87±0.00	−0.10±0.00	0.30±0.00	−0.02±0.00
40	0.42±0.07	1.34±0.01	−0.19±0.00	0.53±0.01	−0.04±0.00
50	0.61±0.09	1.82±0.02	−0.29±0.01	0.80±0.01	−0.06±0.01
60	0.81±0.12	2.28±0.02	−0.40±0.01	1.09±0.02	−0.09±0.01
70	1.02±0.14	2.71±0.03	−0.52±0.02	1.38±0.04	−0.12±0.01
80	1.21±0.16	3.12±0.05	−0.64±0.03	1.67±0.06	−0.15±0.02
90	1.40±0.18	3.51±0.06	−0.77±0.04	1.96±0.08	−0.18±0.03
100	1.57±0.20	3.88±0.07	−0.89±0.05	2.25±0.10	−0.22±0.04
120	1.87±0.22	4.54±0.10	−1.13±0.08	2.79±0.16	−0.28±0.06
140	2.11±0.24	5.12±0.14	−1.37±0.12	3.30±0.23	−0.34±0.08
160	2.27±0.26	5.65±0.17	−1.59±0.16	3.78±0.31	−0.40±0.11
180	2.38±0.28	6.11±0.21	−1.80±0.20	4.22±0.39	−0.45±0.14
200	2.42±0.29	6.53±0.25	−1.99±0.25	4.63±0.49	−0.49±0.17
220	2.42±0.32	6.91±0.28	−2.18±0.30	5.01±0.59	−0.53±0.21
240	2.36±0.35	7.26±0.32	−2.36±0.35	5.36±0.69	−0.57±0.25
260	2.27±0.38	7.58±0.36	−2.53±0.40	5.64±0.80	−0.60±0.28
280	2.14±0.42	7.87±0.40	−2.68±0.46	5.99±0.91	−0.63±0.32
300	1.97±0.47	8.14±0.44	−2.83±0.52	6.28±1.02	−0.65±0.36
320	1.78±0.52	8.39±0.47	−2.97±0.58	6.55±1.13	−0.67±0.40
340	1.56±0.58	8.62±0.51	−3.10±0.63	6.80±1.25	−0.69±0.45
360	1.32±0.64	8.83±0.55	−3.23±0.69	7.03±1.36	−0.71±0.49
380	1.06±0.70	9.03±0.58	−3.34±0.75	7.25±1.48	−0.72±0.53
400	0.73±0.77	9.22±0.62	−3.46±0.81	7.46±1.60	−0.73±0.57

amplitudes with any degree of accuracy. This is because inelastic effects are important at these higher energies, and we have no reliable way of treating the inelasticity. Bearing this fact in mind, we see that any serious attempt to determine the $I=0$ amplitudes accurately at energies above 425 MeV is foredoomed to failure. The (n,p) data are no more complete above 425 MeV than they are below it. The one exception is at

TABLE XIV. Phase-shift values from the 22-parameter 0–750-MeV solution. Only the isotopic spin $I=0$ phases are shown here. The $I=1$ phases are those of Table III in Paper VIII. This solution is discussed in the text. The combined phases give a χ^2 total of 2747 for a fit to 1147 (p,p) data and 901 (n,p) data; thus the M value is 1.34 for the combined solution.

Lab energy (MeV)	$^1P_1$	$^1F_3$	$^3S_1$	ϵ_1	$^3D_1$	$^3D_2$	$^3D_3$	ϵ_3	$^3G_3$	$^3G_4$	$^3G_5$
30	−2.58	−0.58	77.88	−1.21	−3.68	5.23	0.36	0.87	−0.09	0.30	−0.02
60	−6.19	−1.23	58.75	−0.21	−7.98	11.38	1.14	2.28	−0.34	1.07	−0.10
90	−11.32	−1.61	45.57	1.48	−11.11	16.09	1.91	3.51	−0.57	1.92	−0.22
120	−16.50	−1.87	35.44	3.03	−13.49	19.48	2.50	4.54	−0.72	2.71	−0.35
150	−21.09	−2.12	27.45	4.21	−15.53	21.83	2.88	5.40	−0.79	3.40	−0.48
180	−24.86	−2.40	21.09	4.95	−17.48	23.37	3.06	6.12	−0.78	4.01	−0.61
210	−27.80	−2.75	16.02	5.29	−19.51	24.27	3.07	6.74	−0.70	4.54	−0.73
240	−29.96	−3.17	11.98	5.27	−21.68	24.69	2.92	7.27	−0.57	4.99	−0.85
270	−31.44	−3.66	8.79	4.96	−24.04	24.73	2.66	7.74	−0.40	5.40	−0.96
300	−32.31	−4.22	6.29	4.39	−26.60	24.47	2.29	8.15	−0.19	5.75	−1.07
330	−32.67	−4.84	4.37	3.61	−29.34	23.98	1.84	8.52	0.05	6.05	−1.17
360	−32.58	−5.51	2.92	2.67	−32.27	23.31	1.32	8.85	0.31	6.32	−1.27
390	−32.13	−6.23	1.86	1.59	−25.36	22.50	0.74	9.15	0.58	6.55	−1.36
420	−31.35	−6.99	1.14	0.41	−38.60	21.57	0.13	9.42	0.87	6.76	−1.44
450	−30.31	−7.78	0.70	−0.86	−41.96	20.56	−0.52	9.67	1.17	6.95	−1.53
480	−29.05	−8.60	0.50	−2.20	−45.44	19.48	−1.20	9.90	1.47	7.11	−1.60
510	−27.61	−9.44	0.49	−3.59	−49.01	18.36	−1.90	10.12	1.77	7.25	−1.68
540	−26.01	−10.30	0.66	−5.01	−52.65	17.20	−2.61	10.31	2.08	7.38	−1.75
570	−24.28	−11.18	0.96	−6.46	−56.37	16.02	−3.34	10.50	2.39	7.50	−1.82
600	−22.45	−12.06	1.39	−7.93	−60.13	14.82	−4.07	10.67	2.70	7.61	−1.88
630	−20.54	−12.95	1.92	−9.41	−63.94	13.61	−4.81	10.83	3.00	7.70	−1.95
660	−18.56	−13.85	2.53	−10.89	−67.77	12.40	−5.55	10.98	3.30	7.78	−2.01
690	−16.53	−14.75	3.21	−12.36	−71.63	11.20	−6.29	11.13	3.60	7.86	−2.07
720	−14.46	−15.64	3.95	−13.83	−75.49	10.00	−7.02	11.26	3.89	7.93	−2.12
750	−12.37	−16.54	4.75	−15.29	−79.36	8.81	−7.76	11.39	4.18	7.99	−2.18

600–650 MeV, where the Dubna workers have made a valiant effort to provide at least some information on the more complicated neutron scattering experiments. However, this energy is high enough that inelastic effects are very important, and both elastic and inelastic data are still very incomplete even there.

The energy-dependent analysis from 0–750 MeV was carried out in the following manner. The $I=1$ phases were fixed at the values given in Table III of Paper VIII. The $I=0$ phases were treated as being wholly elastic over the entire energy range. Since these phases are prevented by conservation of isotopic spin from coupling to the final-state (3,3) resonance that seems to dominate the $I\approx 1$ inelastic scattering near threshold, the elastic approximation is actually not a bad one for the $I=0$ amplitudes. The only datum we have included on the $I=0$ inelasticity is a total (n,p) reaction cross section at 600 MeV.[9] The experimental value is 8.0 ± 0.6 mb, and the inelasticity coming from the $I=1$ amplitudes of Paper VIII gives a value of 5.5 mb. The remaining 2.5 mb is then what the $I=0$ amplitudes should contribute at 600 MeV. However, Measday[10] has recently reviewed the pion-production data, and he finds that the $I=0$ total reaction cross section at 600 MeV is only about half of the value that we deduced from Ref. 9. Thus the approximation of setting the inelasticity equal to zero for the $I=0$ amplitudes is a reasonable one. Since we found only 95 useful (n,p) data between 410 and 750 MeV, we kept in addition almost all of the low-energy (n,p) data that were used for the 0–400-MeV analysis described above. The data set for the 0–750-MeV searches consisted of 901 data from 14 to 730 MeV.

Phase-shift solutions were obtained using 29, 22, and 19 parameters. The χ^2 values were 1134, 1172, and 1360, respectively. Comparison of the 22- and 19-parameter solutions shows that even though the high-energy (n,p) data are very incomplete, they still reveal a preference for G waves that deviate from those obtained from OPE-contribution values. As we discussed in Sec. IV, the 22-parameter solution includes G waves in the search, whereas the 19-parameter solution does not. The phases for the 29-parameter solution did not differ significantly from those of the 22-parameter solution, even though the χ^2 values were somewhat different. We chose the 22-parameter solution as the most meaningful one to present. Table XIV gives the 0–750-MeV $I=0$ phase-shift values for this solution. In Paper VIII, we did not quote uncertainties for the (p,p) energy-dependent solution above 400 MeV. Therefore, we are not justified in quoting uncertainties for the $I=0$ phases of Table XIV in the present paper. These phases, when used in conjunction with the (p,p) $I=1$ phases, do give a good fit to the available data over the entire energy range, but in energy region above 450 MeV they are in no sense accurately determined.

The combined $I=1$ and $I=0$ phases from Table III of Paper VIII and Table XIV of the present paper

[9] Yu. M. Kazarinov and Yu. N. Simonov, reference Dubna (1965) of Table II.

[10] D. Measday (private communication).

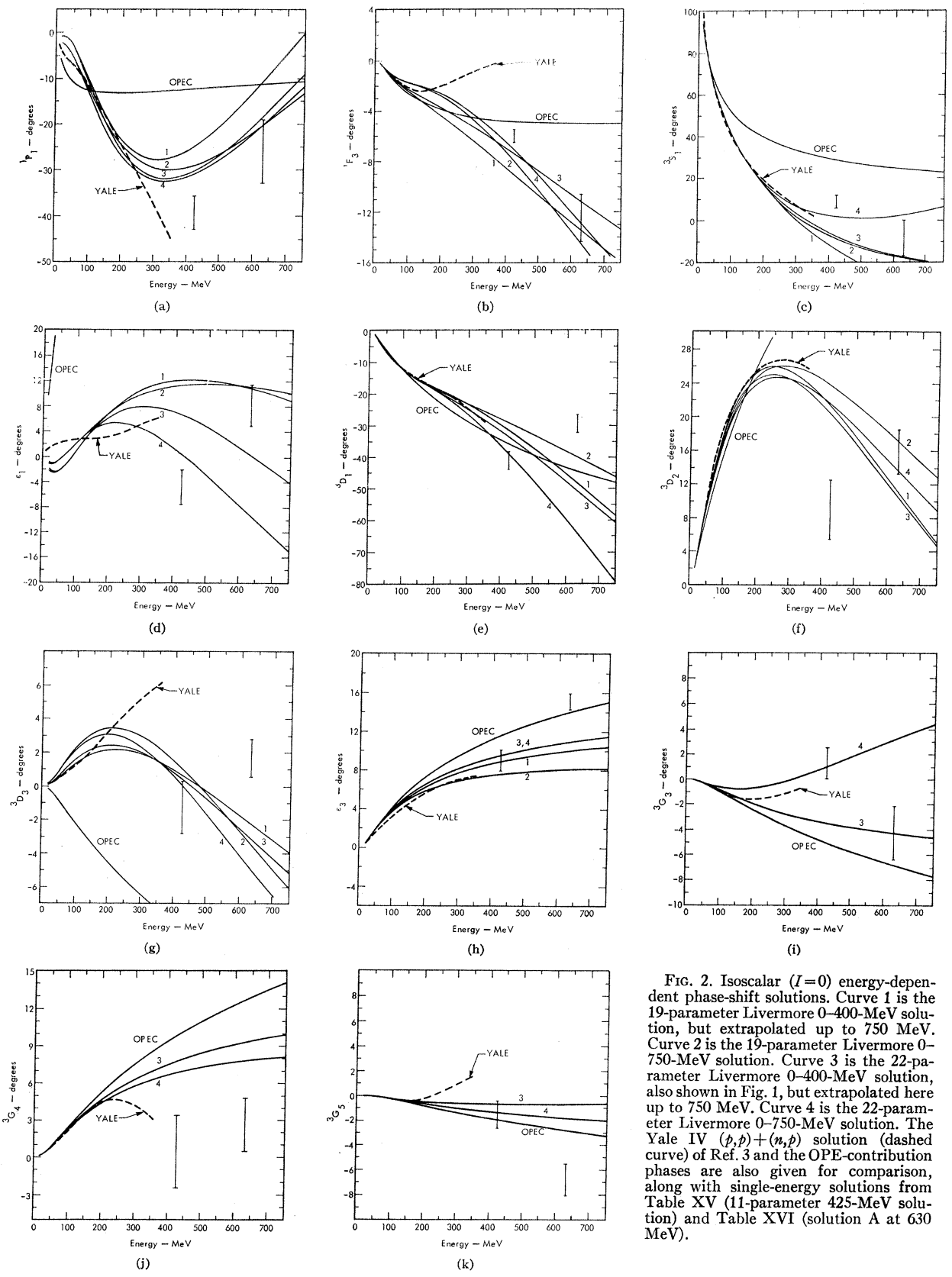

FIG. 2. Isoscalar ($I=0$) energy-dependent phase-shift solutions. Curve 1 is the 19-parameter Livermore 0–400-MeV solution, but extrapolated up to 750 MeV. Curve 2 is the 19-parameter Livermore 0–750-MeV solution. Curve 3 is the 22-parameter Livermore 0–400-MeV solution, also shown in Fig. 1, but extrapolated here up to 750 MeV. Curve 4 is the 22-parameter Livermore 0–750-MeV solution. The Yale IV $(p,p)+(n,p)$ solution (dashed curve) of Ref. 3 and the OPE-contribution phases are also given for comparison, along with single-energy solutions from Table XV (11-parameter 425-MeV solution) and Table XVI (solution A at 630 MeV).

TABLE XV. Isoscalar ($I=0$) phase at 425 MeV. The $I=1$ phases for the energy-independent solutions are those of solution 2, Table V, in Paper VIII. The energy-dependent solutions, shown here for comparison purposes, are those of Tables XIII and XIV in the present paper.

Analysis	Energy-independent			Energy-dependent	
No. of data[a]		30			
Energy range[a]		400–410		912	897
Free phases	8	11[b]	13	7–400	14–730
χ^2 [a]	46.62	22.97	20.48	984	1195
$^1P_1$	−30.57±2.56	−39.44±3.64	−42.39±4.45	−30.5	−31.2
$^1F_3$	−7.15±0.80	−6.01±0.55	−3.89±2.03	−7.4	−7.1
$^1H_5$	(−2.19)	(−2.19)	−3.69±1.34	(−2.2)	(−2.2)
$^3S_1$	−11.27±3.56	8.13±2.90	4.95±6.60	−8.3	1.0
ϵ_1	15.58±2.07	−4.85±2.61	−2.59±3.81	6.4	0.2
$^3D_1$	−27.05±1.61	−41.41±2.90	−38.05±5.29	−33.7	−39.2
$^3D_2$	20.51±1.77	8.65±3.74	12.61±7.69	20.2	21.4
$^3D_3$	2.67±1.19	−1.31±1.69	−0.78±2.53	0.4	0.0
ϵ_3	7.65±0.75	8.98±0.99	8.34±1.74	9.4	9.5
$^3G_3$	(−5.09)	1.18±1.21	−0.65±2.66	−3.6	0.9
$^3G_4$	(9.72)	0.39±3.02	2.60±3.74	7.7	6.8
$^3G_5$	(−2.07)	−1.45±1.13	−0.52±1.52	−0.7	−1.4
ϵ_5	(3.89)	(3.89)	3.67±0.57	(3.9)	(3.9)

[a] (n,p) data only. The $I=1$ amplitudes were held fixed at their values from the (p,p) analyses. The phase shifts are all quoted at an energy of 425 MeV. Phase-shift energy derivatives from the energy-dependent analyses were used in carrying out the "single-energy" analyses.
[b] The 11-parameter solution is favored.

represent a fit to 1147 (p,p) data from 23 to 736 MeV and 901 (n,p) data from 14 to 730 MeV. The χ^2 sum for the 2048 data is 2747, giving an M value of 1.34. 53 phenomenological parameters were used to represent 14 free $I=1$ and 11 free $I=0$ phases.

Figure 2 shows the 19- and 22-parameter $I=0$ phases obtained from the present analysis. It also shows the 19- and 22-parameter $I=0$ solutions of the 0–400-MeV analysis extended up to 750 MeV, the OPE-contribution phases for comparison purposes, and the Yale solution (Y-IV) $pp+np$. The single-energy-solution values above 400 MeV are likewise included, so that the reader can get a general impression of the over-all consistency of the results. The phases below 400 MeV are in rather good agreement, but the need for additional (n,p) data above 400 MeV is clearly apparent.

The single-energy results at 425 MeV are shown in Table XV. The $I=1$ phases from solution 2 of Table V in Paper VII were used, together with 30 (n,p) data at 400 and 410 MeV. Phase-shift energy derivatives were taken from the energy-dependent analysis, and the $I=0$ phases are quoted in Table XV at an energy of 425 MeV. From Table XV we see that G waves must be included in the search if we are to obtain a reasonable value for χ^2. Adding $^1H_5$ and ϵ_5 as free parameters did not materially reduce χ^2. Thus the 11-parameter single-energy solution is probably the most meaningful one. However, when we compare this solution to the values obtained from two versions of the energy-dependent solution to the values obtained from two versions of the energy-dependent solution, we see that the determination of the $I=0$ phases at this energy is only qualitative. The uncertainties quoted for the 11-parameter solution are clearly misleading. Table XI contains the second-derivative and error matrices for the 425-MeV single-energy solution. Table XII shows the $I=1$ and $I=0$ phases for this solution.

The difficulty with an (n,p) analysis at 425 MeV is that the available (n,p) data impose relatively weak constraints on the $I=0$ phases, even when we keep the $I=1$ phases fixed. The only available (n,p) data near 425 MeV are differential cross-section data, polarization data, and total cross sections. With this scarcity of data, a single-energy analysis leads to a χ^2 hypersurface that has many local minima and that is nowhere accurately parabolic. An energy-dependent analysis, on the other hand, becomes inevitably biased by the energy-dependent forms chosen, since the phases are more or less free to follow any constraints imposed by the model. This situation also holds for (n,p) analyses at energies below 425 MeV, since the (n,p) data selection is everywhere incomplete. However, the situation becomes more critical as the energy is increased and the number of phases deviating appreciably from the OPE contribution increases. Finally, at energies where inelastic effects become important, it is difficult to draw any significant conclusions.

With this introduction, we feel rather diffident about quoting any single-energy (n,p) analyses at 630 MeV. However, in the interests of completeness we present Table XVI. The (n,p) data selection near 630 MeV is actually fairly extensive. But our inability to handle the effects of inelasticity in any definite manner, as was described in detail in Paper VIII, means that we do not have reliable values for the $I=1$ phases. Since the $I=1$ and $I=0$ phases are strongly correlated, this in turn means that we can say little about the $I=0$ phases.

Solutions A and B in Table XVI use different sets of $I=1$ phases, as described in the caption. These are true solutions in the sense that a fairly extensive set of

TABLE XVI. Isoscalar ($I=0$) phases at 630 MeV. The $I=1$ phases for solutions A and B are solutions 2 and 3, respectively, of Table VI in Paper VIII. Solution C is from Table XIV of the present paper. The scatter of the results gives a measure of the reliability of the phase-shift determinations.

Analysis	Energy-independent		Energy-dependent
No. of data[a]	77		897
Energy range (MeV)	580–635		14–730
Solution	A	B	C
χ^2 [a]	115.1	114.5	1195
$^1P_1$	−26.38±6.95	−18.54±3.43	−20.54
$^1F_3$	−12.56±1.90	6.88±1.86	−12.95
$^1H_5$	2.20±1.99	(−2.53)	(−2.53)
$^3S_1$	−8.03±7.68	−13.89±3.65	1.92
ϵ_1	7.81±3.34	19.07±1.58	−9.41
$^3D_1$	−29.94±2.83	20.08±3.06	−63.94
$^3D_2$	15.80±2.57	17.41±2.34	13.61
$^3D_3$	1.64±1.15	4.80±1.04	−4.81
ϵ_3	14.99±0.83	14.78±1.28	10.83
$^3G_3$	−4.41±2.10	−3.78±1.34	3.00
$^3G_4$	2.55±2.17	10.33±1.23	7.70
$^3G_5$	−6.87±1.30	−5.33±0.79	−1.95
ϵ_5	8.45±0.79	(5.02)	(5.02)

[a] (n,p) data only.

searches led consistently to these values. However, the solutions differ drastically from one another, and they differ from the energy-dependent solution shown for comparison purposes. Since we could define a large number of $I=1$ solutions in addition to those used here, it is apparent that the solutions of Table XVI are merely representative of a large number of answers that could be obtained by variations in the handling of the $I=1$ or the $I=0$ phases. From the scatter of the values for the phases, it is apparent that the quoted uncertainties in the phases have no validity. And when we superimpose on all of this the fact that we have neglected any of the inelasticity that should rightfully be accorded to the $I=0$ phases at 630 MeV, it is clear that the $I=0$ scattering matrix at 630 MeV is essentially undeterminable at the present time. More (p,p) and (n,p) elastic scattering data are needed, but an equally crucial requirement is for some reliable treatment of the inelasticity.

VI. DISCUSSION

In an energy-independent phase-shift analysis, the low angular momentum phases are treated as free parameters and the high angular momentum phases are represented by their OPE-contribution values. The free phase shifts are obtained by fitting to data in a narrow energy band, and are in no manner related to the data at other energies. The model dependence of such a calculation is held to a minimum, namely, to the use of OPE-contribution phases and the use of fixed local energy derivatives. Phenomenologists who do single-energy phase-shift analyses differ mainly in small details such as the correct number of phases to treat as free parameters. The phase-shift values obtained by these groups are all in general agreement at the present time, at least for the isovector phases.

The situation with regard to energy-dependent phase-shift analyses is more complicated.

In the absence of firm theoretical guidance, such analyses are of necessity based on a rather arbitrary choice of a functional energy dependence for the phase shifts. The energy-dependent forms are chosen with adjustable parameters, with respect to which χ^2 is minimized. The forms should be selected on the basis of physical plausibility, and they must have a flexibility that is consistent with the demands of the data, and yet also with a practical number of free parameters. The question then arises as to the extent to which the phase shifts obtained in an energy-dependent analysis reflect the model used to represent the phases rather than reflect the data. This question is discussed below.

Even though the necessary assumptions lead to limitations in the energy-dependent analyses, there are nevertheless valid reasons for an interest in this kind of analysis. As the Livermore work has demonstrated,[11] plausible energy-dependent forms do exist, so that meaningful energy-dependent analyses are feasible. This is an important consideration in the analysis of (n,p) data, since in general these data are not grouped in sufficient quantity near single energies to permit adequate energy-independent analyses. In this circumstance, some form of energy-dependent analysis is required in order to extract the maximum available information from data spread over a broad energy range.

Another reason is given in the fact that phases obtained from single-energy analyses often exhibit rather erratic behavior when plotted as functions of energy. This behavior reflects either unknown systematic errors or else incompleteness in the data selection. To evaluate these possibilities, we are led naturally to energy-dependent analyses.

Finally, if we wish to investigate the restrictions imposed on a theoretical model by the entire body of nucleon-nucleon scattering data, we need to treat all of the available data simultaneously, which is precisely the function of an energy-dependent analysis. This treatment is also important from a predictive standpoint, such as using the results of present measurements in the planning of future experiments.

The only two groups to carry out large-scale energy-dependent analyses of the nucleon-nucleon data to the present time are the Yale and Livermore groups. Since both groups have now completed energy-dependent analyses that include essentially the entire body of (p,p) and (n,p) elastic scattering data, it seems appropriate to discuss the effects of model dependence on the phase shifts by comparing the results of the Livermore analyses (Papers VII–XI) with the latest Yale analyses.[3]

[11] The suitability of a wide class of such functions has been investigated by R. A. Arndt and M. J. Moravcsik, Nuovo Cimento A51, 108 (1967).

The energy-dependent forms used by the Livermore and the Yale groups are quite different. The Livermore form, which in Paper VII is called form A, has the OPE-contribution phase, which corresponds to the OPE process, as the leading term in the expansion. (In the S waves, we substitute a scattering length and effective-range expansion in place of the OPE-contribution phase.) The other terms are Legendre functions that are chosen to have singularity structures and threshold behaviors appropriate to two-, three-, etc., pion-exchange processes. These forms are well-defined functions, continuously dependent on the same parameters over the entire energy range. There is no joining of different functions, that depend on independent parameters, from one region to another. Using such forms, we can tell precisely how much parameter freedom is really present *and required* in each phase shift. More importantly, we can use matrix techniques to carry out the phase-shift χ^2 minimization, to determine the correlated uncertainties on all of the phases at all energies, and to determine the accuracy with which derived quantities (for example, experimental observables) can be predicted.

The energy-dependent phases used by the Yale workers are constrained to be precisely the OPE-contribution values at low energies. (This is quite different from the Livermore parametrization, since the Livermore phases, though they include the OPE-contribution phase as the leading term, are free to deviate from OPE-contribution even at the lowest energies. Thus the Livermore solution gives a precision fit down to very low energies.) At higher energies, the Yale phases are apparently represented by different functions in different energy regions. To the extent that this is true, the Yale forms must correspond to considerably more parameter freedom than does the Livermore form. From published information, it does not appear to be possible to specify well-defined uncertainties for quantities derived from the Yale results.

If the data selection is reasonably accurate and complete, and if both the Yale and Livermore energy-dependent forms include sufficient freedom, then we would expect both groups to arrive at the same answers. This is the situation for the (p,p) analyses and the isovector amplitudes. However, for the (n,p) analyses, the data are in general neither very accurate nor very complete. In this case it is unavoidably necessary to reduce the amount of allowable freedom in order to obtain a well-defined result. The answer thus obtained will certainly be influenced by the model. A comparison of the Yale and Livermore isoscalar phases at low energies shows this result very clearly.

Table XVII gives a comparison of the isovector phases for the latest Yale solution and for the Livermore energy-dependent and energy-independent solutions below 400 MeV. From XVII, it can be seen that the phase-shift values for all the solutions shown are very similar. The (p,p) data selection below 400 MeV is complete enough that a unique and quantitatively well-determined isovector scattering matrix can be obtained from it.

A comparison in Table XVII between the variations in the phase shifts and the quoted uncertainties in the phase shifts shows that the error limits do have significance. The variations are in many cases more than one listed standard deviation, but they in no case greatly exceed that amount. (This result does not hold for the isoscalar phases at the present time.)

A comparison of the Livermore energy-dependent and energy-independent analyses in Table XVII illustrates the comments concerning uncertainties. The energy-independent uncertainties may be taken to be the maximum uncertainties in the phases allowed by the data. The energy-dependent uncertainties will clearly be smaller, with the decrease dependent on the "stiffness" of the energy-dependent forms chosen, and on the increase in the number of data used. (The uncertainties vary in the same sense as the ratio of free parameters to data, which is usually considerably smaller for energy-dependent than for energy-independent analyses.) In the Livermore energy-dependent analysis shown in Table XVII, we have used a minimum acceptable number of free parameters (23 for 14 $I=1$ phases) which still suffices to give an accurate fit to the data. Thus we might expect considerable model dependence in this solution. In particular, we expect the phase-shift uncertainties thus obtained to underestimate somewhat the true uncertainties. Thus the Livermore energy-dependent and energy-independent uncertainties shown in Table XVII provide lower and upper bounds, respectively, for the "true" uncertainties.

Table XVII also gives the "parallel shift" uncertainties for the Yale Y-IV $pp+np$ solution. At energies below 100 MeV, the Yale uncertainties are comparable to but slightly larger than our *energy-dependent* uncertainties. However, at energies above 150 MeV, the Yale uncertainties are essentially the same as our *energy-independent* uncertainties. This substantiates the belief, expressed above, that the Yale parametrization must implicitly correspond to a considerably larger number of adjustable parameters than the 23 that we used in our energy-dependent solution.

A comparison of the Livermore energy-dependent and energy-independent phase-shift values in Table XVII shows that they are not strongly influenced by our choice of model for the analysis. In addition to the models described here, we have made extensive investigations of other models, both by using form A with a variety of parametrizations, and by using rather different forms. We have verified to our own satisfaction that the results reported here, both the phase-shift values and the uncertainties, are not significantly influenced by our choice of model. The models were of course from the class that we consider physically plausible, and we had to provide in each case a sufficient number of and proper distribution for the adjust-

TABLE XVII. Comparison of isovector ($I=1$) phases for the Yale and Livermore solutions. The solution labeled Yale Y-IV *pp* is from Table II of Ref. 3, and the solution labeled Yale Y-IV *np* is from Table III. The Livermore-EDA solution is from Table V of Paper VII, and the Livermore 0-750 EDA solution is from Table VII of Paper VIII. The Livermore-EIA solution is from Table VI of Paper VII. This comparison is discussed in the text.

Solution	$^1S_0$	$^1D_2$	$^1G_4$	$^3P_0$
		25 MeV		
Yale Y-IV *pp*	48.69±0.01	0.88±0.02	0.05	7.84±0.17
Yale Y-IV *np*	50.52±0.01	0.92±0.02	0.04	8.15±0.17
Livermore-EDA	48.51±0.11	0.77±0.01	0.05±0.00	8.28±0.12
Livermore-EIA	48.61±0.26	0.76±0.03		8.53±0.45
		50 MeV		
Yale Y-IV *pp*	38.56±0.01	1.98±0.02	0.17	11.68±0.17
Yale Y-IV *np*	39.39±0.01	2.03±0.02	0.14	11.75±0.11
Livermore-EDA	38.78±0.13	1.77±0.02	0.17±0.00	11.25±0.20
Livermore-EIA	39.55±0.46	1.74±0.10		10.78±0.69
		140 MeV		
Yale Y-IV *pp*	17.65±0.34	5.12±0.11	0.61±0.05	6.07±0.38
Yale Y-IV *np*	17.91±0.34	5.20±0.11	0.58±0.05	5.85±0.38
Livermore-EDA	17.38±0.26	4.91±0.08	0.71±0.02	6.49±0.25
Livermore-EIA	16.85±0.58	4.88±0.17	0.80±0.07	5.93±0.54
		210 MeV		
Yale Y-IV *pp*	5.73±0.80	7.24±0.18	1.04±0.10	−0.53±0.77
Yale Y-IV *np*	5.88±0.80	7.32±0.18	1.05±0.10	−0.79±0.77
Livermore-EDA	6.05±0.33	6.92±0.12	1.10±0.05	−0.64±0.37
Livermore-EIA	5.59±0.53	7.03±0.29	1.10±0.10	−1.23±0.55
		330 MeV		
Yale Y-IV *pp*	−9.43±1.31	10.49±0.58	1.13±0.27	−13.33±1.41
Yale Y-IV *np*	−9.40±1.31	10.54±0.58	1.15±0.27	−13.64±1.41
Livermore-EDA	−12.30±0.78	9.69±0.22	1.70±0.11	−11.75±0.80
Livermore 0-750 EDA	−9.27	9.45	1.89	−13.76
Livermore-EIA	−10.70±1.46	9.09±0.52	1.20±0.25	−12.40±1.57

Solution	$^3P_1$	$^3P_2$	ϵ_2	$^3F_2$
		25 MeV		
Yale Y-IV *pp*	−4.72±0.06	2.45±0.05	−1.13±0.04	0.12±0.10
Yale Y-IV *np*	−4.96±0.06	2.63±0.05	−1.17±0.04	0.10±0.10
Livermore-EDA	−5.20±0.04	2.75±0.04	−0.87±0.01	0.10±0.00
Livermore-EIA	−5.01±0.21	2.43±0.16		
		50 MeV		
Yale Y-IV *pp*	−7.98±0.06	5.84±0.05	−2.11±0.04	0.39±0.10
Yale Y-IV *np*	−8.23±0.06	6.10±0.05	−2.14±0.04	0.34±0.10
Livermore-EDA	−8.45±0.06	6.02±0.05	−1.76±0.02	0.30±0.01
Livermore-EIA	−8.16±0.31	5.70±0.15	−1.74±0.21	−0.15±0.29
		140 MeV		
Yale Y-IV *pp*	−16.80±0.12	13.63±0.09	−2.87±0.06	0.64±0.15
Yale Y-IV *np*	−17.02±0.12	13.82±0.09	−2.85±0.06	0.65±0.15
Livermore-EDA	−16.70±0.10	13.58±0.07	−2.91±0.05	0.64±0.09
Livermore-EIA	−16.91±0.17	13.63±0.11	−2.85±0.07	0.84±0.27
		210 MeV		
Yale Y-IV *pp*	−21.84±0.38	15.64±0.23	−2.87±0.13	0.61±0.35
Yale Y-IV *np*	−22.07±0.38	15.71±0.23	−2.83±0.13	0.60±0.35
Livermore-EDA	−22.11±0.18	16.15±0.10	−2.73±0.09	0.57±0.16
Livermore-EIA	−22.20±0.32	15.59±0.23	−2.86±0.16	1.33±0.31
		330 MeV		
Yale Y-IV *pp*	−27.81±0.86	15.83±0.56	−2.50±0.40	0.29±0.57
Yale Y-IV *np*	−28.09±0.86	15.78±0.56	−2.46±0.40	0.27±0.57
Livermore-EDA	−30.59±0.39	17.45±0.26	−1.77±0.25	0.19±0.30
Livermore 0-750 EDA	−30.49	17.50	−2.60	0.24
Livermore-EIA	−28.36±1.20	16.18±0.56	−2.54±0.44	0.42±0.57

TABLE XVII. (*continued*).

Solution	$^3F_3$	$^3F_4$	ϵ_4
	25 MeV		
Yale Y-IV *pp*	−0.28±0.06	0.02±0.03	−0.06
Yale Y-IV *np*	−0.23±0.06	0.01±0.03	−0.05
Livermore-EDA	−0.26±0.00	0.02±0.00	−0.06±0.00
Livermore-EIA			
	50 MeV		
Yale Y-IV *pp*	−0.82±0.06	0.08±0.03	−0.22
Yale Y-IV *np*	−0.72±0.06	0.06±0.03	−0.18
Livermore-EDA	−0.75±0.01	0.13±0.00	−0.21±0.00
Livermore-EIA	−0.39±0.39	0.17±0.18	
	140 MeV		
Yale Y-IV *pp*	−1.99±0.14	0.58±0.08	−0.85±0.03
Yale Y-IV *np*	−2.02±0.14	0.65±0.08	−0.79±0.03
Livermore-EDA	−2.04±0.10	0.83±0.04	−0.77±0.03
Livermore-EIA	−2.11±0.17	0.96±0.14	−0.76±0.03
	210 MeV		
Yale Y-IV *pp*	−2.55±0.21	1.48±0.17	−1.02±0.09
Yale Y-IV *np*	−2.57±0.21	1.49±0.17	−1.02±0.09
Livermore-EDA	−2.56±0.17	1.49±0.07	−1.03±0.06
Livermore-EIA	−2.63±0.20	2.09±0.18	−1.02±0.09
	330 MeV		
Yale Y-IV *pp*	−3.74±0.47	3.15±0.30	−1.27±0.28
Yale Y-IV *np*	−3.76±0.47	3.16±0.30	−1.26±0.28
Livermore-EDA	−2.99±0.31	2.58±0.13	−1.25±0.12
Livermore 0-750 EDA	−3.24	2.86	−1.15
Livermore-EIA	−3.54±0.61	2.80±0.24	−0.99±0.29

Solution	$^3H_4$	$^3H_5$	$^3H_6$
	25 MeV		
Yale Y-IV *pp*	0.00	−0.02	0.00
Yale Y-IV *np*	0.00	−0.01	0.00
Livermore-EDA	0.00±0.00	−0.02±0.00	0.00±0.00
Livermore-EIA			
	50 MeV		
Yale Y-IV *pp*	0.03	−0.10	0.01
Yale Y-IV *np*	0.02	−0.07	0.01
Livermore-EDA	0.03±0.00	−0.10±0.00	0.01±0.00
Livermore-EIA			
	140 MeV		
Yale Y-IV *pp*	0.21	−0.57	0.08
Yale Y-IV *np*	0.18	−0.50	0.07
Livermore-EDA	0.20±0.03	−0.57±0.05	0.11±0.01
Livermore-EIA			
	210 MeV		
Yale Y-IV *pp*	0.38±0.23	−0.99±0.15	0.16±0.15
Yale Y-IV *np*	0.35±0.23	−0.92±0.15	0.14±0.15
Livermore-EDA	0.36±0.06	−0.93±0.10	0.25±0.03
Livermore-EIA	0.10±0.23	−1.00±0.20	0.07±0.14
	330 MeV		
Yale Y-IV *pp*	0.87±0.36	−1.67±0.42	0.64±0.23
Yale Y-IV *np*	0.88±0.36	−1.68±0.42	0.64±0.23
Livermore-EDA	0.60±0.17	−1.47±0.27	0.54±0.08
Livermore 0-750 EDA	0.27	−1.08	0.51
Livermore-EIA	1.23±0.34	−1.92±0.52	0.67±0.16

able parameters. The form-A parametrizations gave the lowest χ^2 values for a given number of free parameters.

A comparison between the Livermore and Yale isoscalar phase shifts is presented in Fig. 2. Curve 3 in Fig. 2 is the Livermore 22-parameter 0–400 MeV solution, extrapolated up to 750 MeV. Curve 4 is the Livermore 22-parameter 0–750-MeV solution. (Curves 1 and 2 are the comparable Livermore 19-parameter solutions.) The dashed curve is the Yale Y-IV $pp+np$ solution. The OPE-contribution phases are also shown.

At very low energies, the Livermore and Yale solutions differ principally in the $^1P_1$ and ϵ_1 phases. Although the Livermore energy-dependent parametrization contains the OPE contribution as the leading term, both of these phases deviate strongly from the OPE-contribution at low energies for all of the Livermore solutions. With the thought that the negative values for ϵ_1 at low energies in the Livermore analysis might be caused by a spurious "overshoot" from the higher terms in the energy parametrization that are required to cancel out the strong OPE-contribution amplitudes near threshold, we removed the OPE-contribution term from the ϵ_1 expansion. However as can be seen in Fig. 2(d), the negative values for ϵ_1 at low energies for the Livermore solutions still persist. The single-energy values for $^1P_1$ and ϵ_1 shown in Figs. 1(a) and 1(d) also illustrate the ambiguous nature of the $I=0$ solutions at energies of 50 MeV and below.

We conclude from our (n,p) analyses that there is nothing in the present (n,p) data selection that *requires* $^1P_1$ and ϵ_1 to approximate to OPE-contribution values at energies around (say) 10–25 MeV. The reason that the Yale solutions for these phases do follow an OPE-contribution behavior at these energies is clearly because they are constrained to do so. Whether one wishes to use the Livermore or the Yale version of the $^1P_1$ and ϵ_1 low-energy phases is at this point an arbitrary decision. We believe that one cannot regard either of these solutions as being a final solution. The low-energy (n,p) data are simply not adequate yet to define a unique solution. The Livermore ϵ_1 and $^1P_1$ phases around 25 MeV are a reflection of the existing low-energy *experimental* situation. The Yale ϵ_1 and $^1P_1$ phases around 25 MeV are a reflection of current low-energy *theoretical* opinion, which prescribes that these phases should closely resemble their OPE-contribution values. (However, we know that the ^3P phases differ appreciably from their OPE-contribution values at much lower energies.) The sign of the quadrupole moment of the deuteron indicates that ϵ_1 should be positive at very low energies.[12]

We badly need accurate (n,p) triple-scattering experiments at 25 MeV.

At high energies, there is a difference between the Yale and Livermore isoscalar phases that can be more directly resolved by the existing experimental data. As shown in Figs. 2(a), 2(b), and 2(g), the Yale $^1P_1$, $^1F_3$, and $^3D_3$ phases each have a behavior above 200 MeV that is radically different from the behavior of the corresponding Livermore phases. If we limit ourselves to (n,p) data at energies of 350 MeV and below, then it might be difficult to choose the correct high-energy behavior for these phases. But when we extend the analysis to energies at 425 MeV and above, it seems clear that the energy dependences for $^1P_1$, $^1F_3$, and $^3D_3$ as given by the Livermore solutions are preferred. The uncertainties in the G waves are so large that discrepancies between different solutions for $^3G_3$, $^3G_4$, and $^3G_5$ probably mean very little. While the (n,p) data above 400 MeV are not sufficient to uniquely define an isoscalar scattering matrix, they do impose strong constraints on the scattering amplitudes. In order to obtain good fits to the data above 400 MeV, we used the energy-dependent forms shown in Fig. 2, which also fit the data below 400 MeV. It is a remarkable fact that curves 1 and 3 in Fig. 2, which were obtained by fitting to (n,p) data up only to 400 MeV, give high-energy extrapolations that are very similar to curves 2 and 4, which we obtained by fitting to (n,p) data up to 730 MeV. This indicates that our energy-dependent forms are appropriate. The success in extrapolating the 0–400-MeV solutions is not due simply to form-limiting constraints, since only 19-parameter solutions, which had the same intrinsic freedom as curve 1 in Fig. 2, but which had different distributions of the adjustable parameters among the phenomenological phases, gave very poor extrapolations.

In the energy region 300–400 MeV, we have listed in Table I the fits to the data (the M values) for both of the 22-parameter solutions: the 0–400- and 0–750-MeV solutions of curves 3 and 4, respectively, in Fig. 2. If form-limiting effects in our higher-energy analyses are important, they should be revealed in this energy region. Since solution 3, with no higher-energy constraints, has much more freedom of accommodation in the 300–400-MeV energy region than does solution 4, we might expect the M values for solution 4 to be significantly higher. However, as Table I shows, they are not. This is strong evidence that form-limiting effects are not important in solution 4 at the intermediate energies, and of course are therefore not important in solution 3 at these energies. Thus we believe that the phase-shift energy dependences above 300 MeV as shown by the Livermore results in Fig. 2 are qualitatively correct.

There is one more difference between the Yale and Livermore procedures that should be mentioned here.

TABLE XVIII. Examination of charge-dependent effects in the $^1S_0$ phase shift. The calculated differences are from the Yale potential model.[a] The "experimental" differences, which are for a somewhat different quantity, indicate that the data are not yet accurate enough to be sensitive to this refinement in the analysis.

Energy (MeV)	Calculated differences[a] $(^1S_0)p,p-(^1S_0)n,p$	"Experimental" differences[b] $(^1S_0)p,p-(^1S_0)p,p+n,p$
25	$-1.82°$	$+0.01°\pm0.36°$
50	$-0.83°$	$+0.03°\pm0.63°$
95	$-0.41°$	$+0.65°\pm1.89°$
142	$-0.26°$	$-0.15°\pm0.80°$
210	$-0.15°$	$+0.06°\pm0.74°$
330	$-0.03°$	$+0.24°\pm2.06°$

[a] Calculations by the Yale group (Ref. 3).
[b] Obtained from Table VI of Paper VII and Table IV of the present paper.

[12] G. Breit and R. D. Haracz, in *High Energy Physics*, edited by E. H. S. Burhop (Academic Press Inc., New York, 1967), Vol. I, Chap. 2, footnote 15, pp. 127–128.

In their recent paper, the Yale group[3] treated the combined (p,p) plus (n,p) analysis by precalculating from a potential model the differences to be expected between the (p,p) $I=1$ phases and the (n,p) $I=1$ phases, and then fixing this difference in searching against the combined (p,p) plus (n,p) data. That is, they used a specific charge-dependent assumption. The largest splitting is expected in the $^1S_0$ phase. In Table XVIII we have listed the expected difference, $(^1S_0)(p,p)-(^1S_0)(n,p)$, as calculated by the Yale workers, together with the "experimental" values that we obtained from the single-energy solutions of Table IV for $(^1S_0)(p,p)-(^1S_0)(p,p+n,p)$. These are not equivalent quantities, and we expect our experimental differences, so defined, to be roughly half as large as if we had really used independent $^1S_0$ phases for (p,p) and for (n,p). However, the sign should still be the same. As we can see from Table XVIII, at five of the energies the sign obtained experimentally is the opposite of that expected theoretically. The sign of this difference as calculated theoretically is surely correct, since the Coulomb repulsion in the (p,p) case at low energies serves to keep the nucleons apart and weaken the nuclear attraction. Thus our conclusion is that the experimental uncertainties are so large in a single-energy analysis that they mask effects due to small violations in the charge-independence hypothesis.

Our energy-dependent analysis, however, may possibly reflect the nonequivalence of the (p,p) and (n,p) $^1S_0$ phases. In fitting to total (n,p) cross sections at low energies, we consistently obtained solutions that agree with the measurements of BSSTH,[5] and that therefore are below the values measured by several other groups,[6] as discussed in Sec. II. If we, in accordance with the recent Yale analysis,[3] had used a larger value for $^1S_0$ (n,p) than for our (fixed) value of $^1S_0$ from the (p,p) analysis, we would have obtained larger values for our calculations of low-energy total cross sections. Since the experimental uncertainties that we are discussing here produced changes in the S phases that are of the same magnitude as uncertainties that already exist in these phases from other sources, this point does not have an important bearing on the present analyses.

Given the existing experimental (n,p) data, it makes no practical difference whether one invokes complete charge independence, as we have done, or else invokes a slight charge dependence, as the Yale group has done in its latest work.[3] The Yale work is useful in calling attention to a refinement that may be significant in future analyses.

VII. CONCLUSIONS AND OBSERVATIONS

Papers VII–IX summarize the work of our group at Livermore in determining phase shifts from the (p,p) and (n,p) scattering data. It is our belief that the (p,p) data below 400 MeV are complete enough and accurate enough to define a quantitatively correct set of scattering amplitudes over the entire elastic energy region. At the higher energies, however, where inelastic effects become important, we find that the elastic amplitudes depend markedly on the treatment accorded the inelastic amplitudes. And since there is as yet no way to adequately handle the inelasticity, we believe that the isovector scattering amplitudes cannot be accurately determined at the present time at energies appreciably above 425 MeV.

Although the threshold for pion production is at 280 MeV, the effect of inelastic scattering seems to be very small at energies up to at least 425 MeV. As we showed in Paper VIII, the very accurate and complete (p,p) measurements at 425 MeV do not *require* that we include any inelasticity at that energy, although the measured total reaction cross section can be used as a constraint on a degree of inelastic freedom accorded to the $^1D_2$ phase.

At energies well above 425 MeV, inelastic effects become very large. At 650 MeV, the inelastic and elastic cross sections in (p,p) scattering are of comparable magnitude. To determine the elastic scattering matrix at 650 MeV purely from elastic scattering processes, we know that nine different kinds of experiments are required at each angle. If we can treat the inelasticity in some reliable manner, which means that we can say something about the unitarity relations for each of the partial waves, then we can get by with fewer than nine independent experiments. Since at the present time we have neither nine experiments nor a reliable model for the inelasticity, we can make no unambiguous determination of the isovector amplitudes at 650 MeV. [It follows, of course, as discussed in the next paragraph, that we can therefore determine very little about the amplitudes at high energies when we carry out combined (p,p) plus (n,p) analyses.]

With regard to the (n,p) data, these can be analyzed at present only by using the results of (p,p) analyses, which essentially fix the isovector amplitudes. The existing (n,p) data give little information about the isovector amplitudes, but when used in conjunction with known isovector amplitudes and the assumption of charge independence they can provide considerable information about the isoscalar amplitudes in the elastic energy region. However, at energies below 50 MeV, even this procedure is not adequate to define unambiguous isoscalar amplitudes from the existing (n,p) data. Until more complete (n,p) data are provided at low energies, it will not be possible, in our opinion, to accurately determine even the low angular momentum isoscalar phases near threshold.

At intermediate energies up through 200 MeV, the isoscalar amplitudes from the various analyses seem to be in reasonable agreement. At energies around 140 and 210 MeV, there exist a number of (n,p) triple-scattering measurements. Since these measurements were obtained largely through the use of deuterium targets, the data thus obtained have systematic errors

that are somewhat difficult to estimate. However the experience with the (p,d) R_T measurement at Rochester,[8] in particular, suggests that the theoretical corrections have been reliably handled.

One useful result that does come out of high-energy analyses is that some information is obtained about the proper high-energy extrapolation of the low-energy analyses. Although there are serious solution ambiguities at 650 MeV, only certain classes of solutions will give good statistical fits to the experimental data at this energy. And if an energy-dependent form for the phase shifts is chosen that provides a reasonable energy variation over the entire energy span, the classes of solutions that fit the data at 650 MeV will give an indication of the allowable energy variations at, say, 300 MeV. It appears to us that the energy-dependent form used in the Livermore analysis is a good one from this standpoint. Thus we conclude that the $^1P_1$ and $^3D_3$ isoscalar phases must decrease in magnitude at energies above 200 MeV, and that the $^1F_3$ isoscalar phase continues toward more negative values at high energies. These results are in contrast to the Yale findings, as shown in Fig. 2.

As far as improving the nucleon-nucleon analyses is concerned, there is a need for more complete (n,p) data, particularly at energies below 100 and above 200 MeV. At energies above 400 MeV, definitive results will be difficult to obtain for either (p,p) or (n,p) scattering until better means are available to handle inelastic effects. Computationally, large-scale computers can now handle all of the available nucleon-nucleon data simultaneously. With matrix search techniques, searching on 100 or more phase-shifts and data-normalization parameters simultaneously is no problem. An interesting point to investigate in future nucleon-nucleon analyses will be the deviations from charge independence of the isovector phases, and in particular the $^1S_0$ phase. The recent Yale analysis,[3] in which the splitting was calculated from a potential model, is an interesting first step. If this splitting can instead be deduced by using a suitable form that contains an adjustable parameter, then this parameter can be included in the search problem, and the nucleon-nucleon data can be used directly to determine any deviations from charge independence.

Another point that should perhaps be considered in more detail is the use of one-boson-exchange potentials to add to the OPE potential already used in the analysis. Although one-boson-exchange potentials taken in Born approximation can by themselves provide a surprisingly good description of the nucleon-nucleon phases (except for S waves) over the entire elastic energy region,[13] we showed in Paper VIII that a "modified modified" phase-shift analysis, using amplitudes from a one-boson-exchange in addition to OPE-contribution, did not result in an improvement in the analysis. Just why this should be the case is not exactly clear.

[13] R. A. Arndt, R. A. Bryan, and M. H. MacGregor, Phys. Letters **21**, 314 (1966); Phys. Rev. **152**, 1490 (1966).

The determination of nucleon-nucleon phase shifts is of course not an end in itself. The phase shifts are merely a translation into quantum-mechanical amplitudes of the experimental observables. The real interest in the phase shifts is for their application in evaluating theoretical models of the nuclear force, first for a system of two nucleons, and then ultimately for a system of more than two nucleons. In this regard, an energy-dependent phase-shift analysis is of interest from the standpoint of the theoretical information that can be obtained from the phase-shift energy dependences deduced from the fit to the data. In our energy-dependent form, we used functions that have proper threshold behavior[14] and that have singularities whose locations are in general agreement with the dictates of the Mandelstam representation. We were not able to obtain any information by this procedure about the discontinuities in the left-hand singularities (in an energy diagram) that represent the 2π and higher exchange processes. However, the energy-dependent forms that we used enabled us to obtain quantitative fits to the data with a minimum number of free parameters. Using 25 $I=1$ and $I=0$ searched phase shifts as represented by only 45 phenomenological parameters plus the OPE-contribution amplitudes, we were able to obtain a precise fit (χ^2 per datum$=1.08$) to our selection of (p,p) plus (n,p) scattering data in the energy range from roughly 2 to 400 MeV. This is a much better fit with this small a number of phenomenological parameters than has been obtained in any other work to date. Furthermore, the solutions thus obtained extrapolate smoothly up to the higher energies above 400 MeV. This is, in our opinion, a remarkable success for the energy-dependent model that we have used. While further work on energy-dependent forms is certainly required, the use of forms with proper singularity structure and threshold behavior seems to lead to functions having realistic energy dependences.

We would like to see the pion-nucleon data analyzed in the same manner that we have analyzed the nucleon-nucleon data. If strict statistical analyses are used to optimize the adjustable parameters over the whole energy range simultaneously, then and only then can reliable estimates be obtained about the experimental uncertainties in the pion-nucleon amplitudes. And, what is possibly equally important at the present time, only in this manner can observables with uncertainties be reliably calculated for use in planning future experiments. It seems to us that some pion-nucleon phenomenologists are not yet using the available computational techniques to best advantage. In a somewhat similar vein, we believe that potential modelists who fit to nucleon-nucleon scattering data should use the available statistical techniques to evaluate the results of their efforts. The free parameters of the potential models should be assigned correlated statistical un-

[14] M. H. MacGregor, Phys. Rev. Letters **12**, 403 (1964).

certainties obtained from fits to the data. Only by this procedure can we tell, for example, just what information about the repulsive core is really contained in the low-energy nucleon-nucleon data. And statistical methods such as these must be used when one tries to deduce the build-up in statistical uncertainties concomitant with moving off the energy shell.

In the present paper, we have listed second-derivative and error matrices for the single-energy (p,p) plus (n,p) solutions at 25, 50, 95, 142, 210, 330, and 425 MeV. These matrices contain, as we showed in detail in Paper VII, most of the information content of the entire body of nucleon-nucleon scattering data below 450 MeV. Fitting theoretical nucleon-nucleon models to these matrices is much simpler and quicker than fitting directly to the data. And for almost all purposes it is fully as accurate. A model that gives a precision fit to the matrices will give a precision fit to the actual data. We strongly urge potential modelists to familiarize themselves with the use of these matrices. The relevant equations for the use of these matrices are given in the Appendix.

The energy-dependent phase shifts and errors that we have provided are useful in checking certain matters such as data consistency, and for interpolating and extrapolating the single-energy results. But since the energy-dependent results quoted here only display the correlated diagonal errors, they are not of much use in a quantitative calculation. We have, of course, parameters and an error matrix that accurately define the scattering over the entire elastic energy range. But such a matrix is too ponderous to reproduce here to the required number of significant figures, and is, unfortunately, of limited use in any case. It is not useful in fitting to models, but only in predicting the accuracy of quantities functionally derived from the associated parameters. The collection of single-energy which matrices we have included, when taken together, contain most of the information content of the parameter matrix, and they are much simpler in practice to use.

A major advantage in the use of matrix representations of the data and matrix techniques in linearized least-squares fitting is that computers of only moderate size suffice and are simply applied to the task. Without matrix techniques, computation problems of the scope that we have described here cannot be treated, other than superficially, without requiring complex application of the largest computers.

ACKNOWLEDGMENTS

We would like to thank D. Cheng, L. Azhgirey, Yu. Kazarinov, G. Stoletov, R. Wilson, B. Rose, J. Perring, J. Simmons, and E. Thorndike for helpful communications about the handling of the (n,p) data. With the publication of the present paper, we complete a decade of effort at Livermore on the determination of the nucleon-nucleon scattering matrix. We would like to acknowledge the many contributions of M. J. Moravcsik, H. P. Noyes, and H. P. Stapp, who were actively involved in the early stages of this program. We would also like to acknowledge the encouragement and support of this work at Livermore by the late Dr. T. Merkle, the late Dr. Mark Mills, and Dr. S. Fernbach.

APPENDIX: EQUATIONS FOR USE OF SINGLE-ENERGY MATRICES

The second-derivative matrices of Tables V–XII are given in units of deg^{-2}. The error matrices of Tables V–XII are given in units of deg^2. The second-derivative matrix at energy E is defined by the equation for the components

$$\alpha_{ij}{}^E=\tfrac{1}{2}(\partial^2\chi^2/\partial\delta_i{}^E\partial\delta_j{}^E), \tag{1}$$

where $\delta_i{}^E$ and $\delta_j{}^E$ are phase shifts. The labels i, j represent the (l,J,S) quantum numbers for the phase shifts. If we take a model that predicts phase shifts $D_i{}^E$, $D_j{}^E$, then the fit that the model would give to the data can be calculated from the equation

$$\chi^2=\sum_E\sum_{i,j}\alpha_{ij}{}^E(D_i{}^E-\delta_i{}^E)(D_j{}^E-\delta_j{}^E). \tag{2}$$

Using the second-derivative matrices $\alpha_{ij}{}^E$ is essentially equivalent to using the data directly. The phase shifts δ^E which should be used with the second-derivative matrices α^E are given in Table XII.

The error matrices are useful in calculating theoretical errors on observables. Given a quantity Q, we can define the gradient vector by its components,

$$\beta_j=\partial Q/\partial\delta_j. \tag{3}$$

The theoretical uncertainty in Q, as given from the present analysis, is then

$$\Delta Q=(\beta^T\alpha^{-1}\beta)^{1/2}, \tag{4}$$

where β^T is the transpose of the gradient vector and α^{-1} is the error matrix. The quantity Q can be any function of the phase shifts, for example any of the standard nucleon-nucleon observables. If we let Q represent one of the phase shifts δ_j, then the gradient vector reduces to the Kronecker delta, and we get the well-known result

$$\Delta\delta_j=(\alpha_{jj}{}^{-1})^{1/2}. \tag{5}$$